Exploration of Small-Scale Solid-State Additive Manufacturing for the Repair of Metal Alloys

Ryan B. Gottwald

Thesis submitted to the faculty of the Virginia Polytechnic Institute and State University in partial fulfillment of the requirements for the degree of

Master of Science
In
Materials Science and Engineering

Hang Z. Yu, Chair
Lei Zuo
Carlos Suchicital

December 13, 2022
Blacksburg, Virginia

Keywords: Additive Manufacturing, Solid-State, Repair, Small-Scale, Steel, Metal

Exploration of Small-Scale Solid-State Additive Manufacturing for the Repair of Metal Alloys

Ryan B. Gottwald

ABSTRACT

When possible, repair of complex metallic components has long been the job of conventional welding techniques. Many alloys used today are difficult to weld, resulting in component and monetary waste when a part needs to be replaced. Fusion-based additive manufacturing methods have gained some ground on the scene of repair by offering an avenue to place material accurately. However, they still lack the ability to process many alloys. Conversely, solid-state manufacturing techniques can process non-weldable alloys but are currently incapable of precisely placing small amounts of material that can be required for component repair. To address this gap, a small-scale solid-state additive manufacturing machine was created from a low-cost desktop mill. It was instrumented with various sensors capable of monitoring the process in-situ. The device was tested with three alloys with varying processing temperatures: aluminum, steel, and a nickel super-alloy. The results from these depositions are promising and show a clear path toward making solid-state additive manufacturing a mobile repair technology.

Exploration of Small-Scale Solid-State Additive Manufacturing for the Repair of Metal Alloys

Ryan B. Gottwald

GENERAL AUDIENCE ABSTRACT

As parts in any device age, something inevitably breaks. When dealing with a broken metallic part, one can either replace it or repair it. Repairing is generally preferred so long as it is not too costly. Unfortunately, repairing a component is often more expensive due to the material being difficult to work with or the geometry being too intricate to fix. Additive manufacturing, commonly known as 3D printing, allows precise placement of material to build a part and has allowed the repair of complex parts. However, some materials are severely weakened using traditional additive manufacturing technologies, which melt small amounts of material and force it to cool in place quickly. To combat this, methods that do not require the material to melt could be used. Currently, these methods place a large amount of material at once, causing significant waste if the excess needs to be removed. Therefore, this work aims to create a small-scale device using a traditional milling machine. It was shown to be capable of placing small amounts of material while offering the advantage of not melting the metal. In the future, it could provide an avenue to repair previously unreachable.

Exploration of Small-Scale Solid-State Additive Manufacturing for the Repair of Metal Alloys

Ryan B. Gottwald

Acknowledgments

I would like to than my mentor and advisor, Dr. Hang Yu, an associate professor in Materials Science and Engineering at Virginia Tech, for his encouragement and interest in my work throughout my collegiate career. His support and guidance throughout these years allowed me to accomplish everything laid out here.

I would also like to thank my committee members, Dr. Lei Zuo and Dr. Carlos Suchicital, for their help in my degree and sticking with me throughout my somewhat tumultuous path through graduate school.

I thank the entirety of the Yu group, both past and present, for their tutelage and for helping me understand many materials science concepts with which I wasn't familiar. Additionally, their existing wealth of knowledge on solid-state processes proved invaluable to my research.

Finally, I would like to thank my friends and family for supporting me through graduate school and giving me guidance and encouragement to seek higher education.

Attributions

Manuscript 1: *Solid-State Metal Additive Manufacturing for Structural Repair*

Author Contributions:

Ryan B. Gottwald wrote the majority of the original draft and performed a majority of the final edits for the final manuscript. This included the bulk of the literature review and drawing comparisons and conclusions for the manuscript. The majority of the figures were either found or created by Ryan.

R. Joey Griffiths added clarification and further research for the AFSD sections of the manuscript. He helped with proofreading the manuscript, ensuring the information's accuracy, and gathering some images for the final section on legacy infrastructure.

Dylan T. Petersen performed some initial literature review on the background of non-solid-state repair. He also helped write these sections for the original draft.

Mackenzie E. J. Perry helped clarify and focus the scope of the manuscript with her experience in repair and helped edit the final draft.

Hang Z. Yu was very active in the manuscript's editing stages, added significant insight into the solid-state processes, and helped guide the topics covered.

Manuscript 2: *Transforming a Desktop Mill for Miniaturized Solid-State Metal Additive Manufacturing*

Author Contributions:

Ryan B. Gottwald performed the entirety of the project work presented in this paper, the only exception being the microscopy of the deposited samples. The work to transform a conventional mill into a platform capable of solid-state deposition was conceived and executed by Ryan. He determined the optimal machine parameters for the chosen material system and solely performed the test depositions presented in this manuscript. He created all of the tables and figures shown. Ryan wrote the original draft, and most of the findings and explanations presented were his work.

Nikhil Gotawala, in combination with Donald Erb, performed the characterization for the samples in this manuscript. He helped edit the results section and provided insight into steel microstructure systems.

Donald Erb helped characterize the samples made by the machine described in this manuscript. He also helped draft the manuscript section describing the findings from this characterization.

Hang Z. Yu helped edit the original draft of this manuscript to refine its scope and improve clarity. He also provided guidance on the basics of solid-state deposition near the beginning of this project and overall oversaw the progress and gave input when needed.

(Space intentionally left blank)

Table of Contents

Chapter 1: Introduction 1

1.1 Motivation for Repair 1

1.2 Solid State Additive Manufacturing Mechanisms 2

Chapter 2: Solid State in Repair 6

2.1 Manuscript 1 6

Introduction 8

Structural Repair by Fusion Welding and Fusion-Based Additive Manufacturing 11

Feasible Solid-State Metal Additive Manufacturing Processes for Repair 14

Evaluation of Repair Capabilities Based on Key Metrics 22

Niche Repair Applications of Solid-State Metal Additive Manufacturing 29

Conclusions and Future Perspectives 31

Manuscript 1 References 33

Chapter 3: Custom Machine Design and Downscaling 38

3.1 Manuscript 2 38

Introduction 39

Machine design and instrumentation 41

Material deposition and characterization methods 44

Results 45

Conclusions and future perspectives 49

Manuscript 2 References..... 49

3.2 Other Material Systems..... 50

3.3 Feeding Mechanism Upgrades..... 55

Chapter 4: Conclusions and Future Work..... 58

References..... 60

Chapter 1: Introduction

1.1 Motivation for Repair

Concerning structural materials, metallic alloys are some of the most common due to their high strength, toughness, and ease of fabrication. As time goes on, the parts we design grow increasingly complex, causing the cost of these components to increase. While the failure of a part does not usually render the entirety of the features useless, it is often that any damage will result in the whole part's replacement. This replacement is often a matter of convenience or cost savings due to such repairs usually needing to be performed by hand [1]. Historically, repair has only been attempted using welding-based methods such as gas arc metal welding, shielded metal arc welding, and others [2]. While cheap, welding results in a relatively large amount of material deposited, which must be removed to return the part to its original form.

Additionally, many alloy systems, such as most engineering aluminum and magnesium alloys, are not receptive to standard melt-based repair methods due to solidification cracking [3, 4]. Even in highly weldable alloys, which include most steels, the base material of the repair is altered due to prolonged thermal exposure from the nearby molten weld [5]. This heat-affected zone is often weaker than the original material and could lead to future mechanical issues, which lead to repeated part failure.

To address some of these issues, additive manufacturing has recently come into the spotlight to repair metallic components [6]. Using additive manufacturing can drastically reduce the excess material needed for repair. This reduction is especially true for technologies that use a powder feed material like laser engineered net shaping (LENS) [7, 8], which have melt pool sizes in the range of 0.5 mm deep [9]. Compared to conventional welding, whose molten pool is 3-6

mm wide and 0.7-5.8 mm deep [10], less material is wasted when repairing finer features. However, melting-based additive manufacturing approaches have the same issues as mentioned previously, namely hot cracking in some alloy systems and thermal softening in the surrounding material. In fact, these additive manufacturing processes can make some aspects of the repair worse due to their extremely high cooling rates of up to 10^4 K/s [11], which further exacerbates issues with melting and solidification.

1.2 Solid State Additive Manufacturing Mechanisms

To fill these gaps in repairable components, technologies have arisen that do not rely on melting. Some well-known examples include friction stir welding and friction stir processing [12]. However, these technologies are non-additive, so they are often only employed for crack repair where no material has been lost. For restoring lost material, additive approaches must be used. These mainly include novel technologies such as cold spray additive manufacturing (CSAM) [13] and additive friction stir deposition (AFSD) [14].

CSAM, seen below in **Figure 1**, uses high-pressure gas to accelerate fine powder into a substrate at an extremely high speed. The kinetic energy contained in the powder causes it and the surface of the substrate to deform and lock together [15]. Machine operators can control the thickness, width, and density of the deposited powder layer by varying the pressure and temperature of the gas as well as the lateral nozzle speed, spray angle, and spray distance. Thermal and solidification issues are avoided by not requiring the powder to melt. All metals are capable of yielding under sufficiently high pressures, so the material library for CSAM is seemingly vast. Unfortunately, not all metals deposit as well as others. Because the mechanism for bonding is dictated by the kinetic energy on impact overcoming the yield strength of the material, alloys with low strength-to-weight ratios are preferable. This makes metals like copper preferable and causes

alloys of metals like titanium to be quite porous due to spherical powders not consolidating [16, 17]. Post-deposition processes like hot isostatic pressing can mitigate these issues [18]. However, this will not fully densify the deposit, requires extra steps, and cannot be used on all repair geometries.

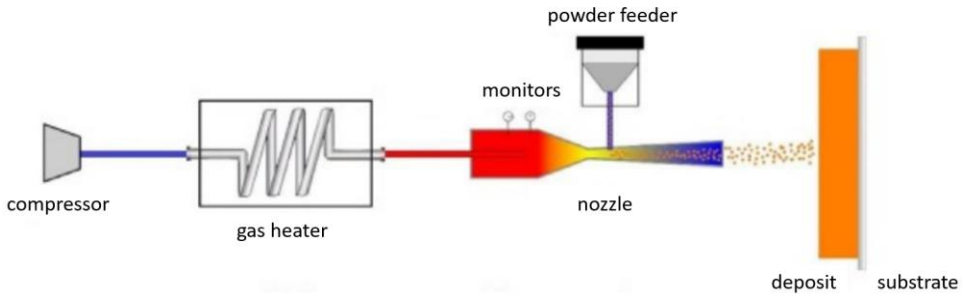

Figure 1. CSAM schematic showing all significant components [19].

Compared to CSAM, AFSD commonly uses a solid square feed rod spun inside a hollow tool. **Figure 2** shows a schematic of this process. A linear actuator applies downward pressure on the feed rod while a motor spins the tool and feed rod together. This generates heat by friction between the substrate and the bottom of the feed rod. Once the feed rod is sufficiently hot, the downward force overcomes the strength of the bottom of the rod, causing it to yield. This plasticized material then flows beneath the tool and mixes with the substrate's top layer, forming a strong metallurgical bond [20, 21]. While this process requires robust machinery to maintain the thousands of newtons of force to yield the feed rod compared to the relatively lightweight CSAM setup, AFSD produces fully dense deposits without any post-process treatments [22, 23].

The use of these technologies for repair will be well explored in Manuscript 1 in Chapter 2. Their advantages in several repair metrics were analyzed, including structural integrity, portability, available materials, repairable geometries, geometric precision, and corrosion resistance. Specifically, on the topic of geometric precision, these technologies typically have large

material deposition tracks. While very useful for repairs of large features, this, unfortunately, causes some of the issues that additive manufacturing for repair initially sought to address. Additionally, these devices are relatively immobile, limiting repairable parts to components that can be removed and relocated.

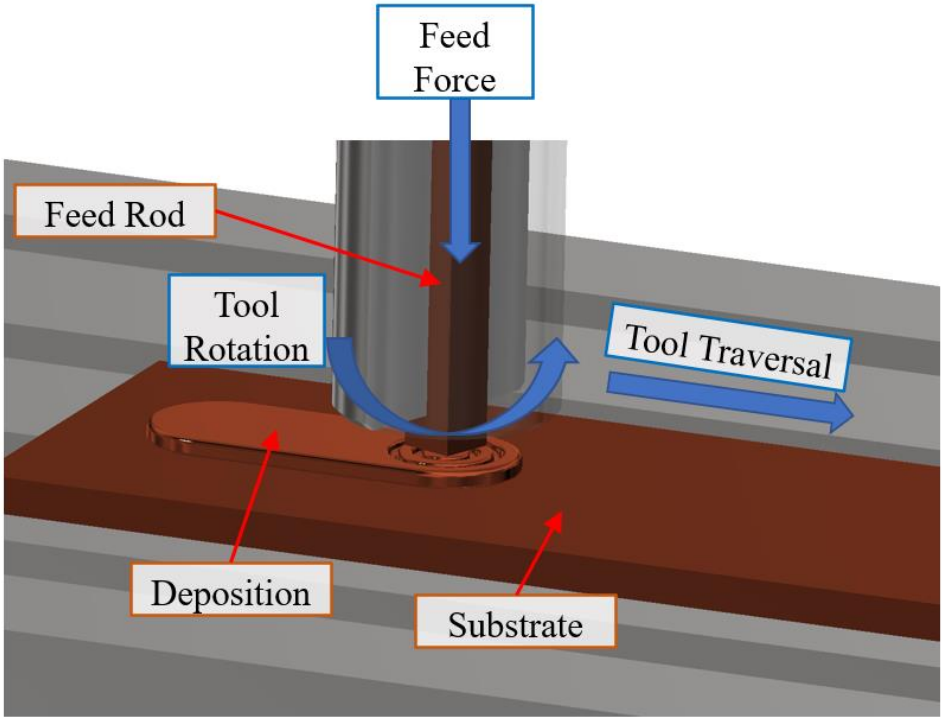

Figure 2. AFSD schematic showing the major components as well as the general operating procedure.

To address these issues, a project was conducted to create a downscaled solid-state additive manufacturing machine capable of using solid feed rods and producing a thin material deposition track. A conventional milling machine was modified with custom components to enable additive deposition or solid feed rods. If successful, this should reduce material waste for thin repair profiles and potentially lighten the assembly enough to allow for mobile repair applications. A few preliminary tests were done to assess the usefulness of this machine using several alloys of substrates and feed rods. The details of this machine and some initial testing using steel alloys are captured in Chapter 3 and Manuscript 2. Alongside this, a few other material systems were tested,

including conventionally easy-to-deposit materials such as aluminum in addition to high-strength, high-temperature nickel-based alloys. Based on these results, future modifications were made to the milling machine to improve future performance, and future work using these upgrades was suggested.

(Space intentionally left blank)

Chapter 2: Solid State in Repair

The following review paper was written to explore the current state of repair and how solid-state additive manufacturing can fit in. Most relevantly, the advantages and existing use cases for solid-state additive manufacturing approaches were explored. This review paper is pasted in the journal format to which it was submitted.

2.1 Manuscript 1: Solid-State Metal Additive Manufacturing for Structural Repair

Solid-State Metal Additive Manufacturing for Structural Repair

Ryan B. Gottwald, R. Joey Griffiths, Dylan T. Petersen, Mackenzie E. J. Perry, Hang Z. Yu *

Department of Materials Science and Engineering, Virginia Tech, Blacksburg, VA 24061, USA.

* Corresponding Author: hangyu@vt.edu

Conspectus

Structural metal components play a vital role in a broad range of industries, from aerospace and automotive to infrastructure and defense. In service, these components can experience substantial wear, thermal fatigue, erosion, corrosion, or chemical reactions, resulting in significant surface or even volumetric damages. Replacement of these components is often energy-intensive and economically impractical. Structural repair, which aims to restore the original geometry while enabling good mechanical performance post-repair, can offset the costs dramatically. Depending on the bonding mechanisms and additive capabilities, structural repair technologies can be divided into four categories: non-additive, melting-based; non-additive, non-melting-based; additive, non-melting-based; additive, melting-based. Although melting-based approaches can be applied to various repair geometries with good precision, the underlying melting and solidification processes inevitably lead to crucial problems impacting the mechanical performance, such as solidification

porosity, high residual stresses, dendritic microstructure formation, elemental segregation, hot cracking, and stress corrosion cracking. To fundamentally solve or minimize these problems, one may employ solid-state technologies that leverage ultrasonic vibration, friction stirring, or particle impact to facilitate metallurgical bond formation. For robust geometry restoration, an additive capability needs to be incorporated for continuous material feeding and precise deposition path control. Currently, two solid-state technologies satisfy the requirement, cold spray and additive friction stir deposition.

In this Account, we discuss the structural repair enabled by solid-state metal additive manufacturing, focusing on (i) cold spray, which is a relatively established process, and (ii) additive friction stir deposition, which is an emerging process recently triggering significant research efforts—the authors are particularly invested in this process and are pioneering the research on process fundamentals and structural repair applications. In cold spray, a substrate is bombarded with small metal particles of high speed; upon impact, the particles and substrate co-deform, resulting in interfacial bonding and mechanical interlocking. In additive friction stir deposition, frictional heat is created after the rapidly rotating feed-rod contacts the substrate, followed by co-plastic deformation and mixing between the deposited material and substrate surface. This renders a strong interface with complex 3D features. Both cold spray and additive friction stir deposition can be applied to a wide range of repair geometries while preventing hot cracking and high thermal exposure. Although cold spray has better portability and spatial resolution than additive friction stir deposition, we believe that additive friction stir deposition is the top choice for repairing load-bearing components given its unparalleled capabilities of rendering equiaxed microstructures and wrought-like mechanical properties. Regarding niche repair applications, cold spray is particularly suited for field repair of surface damages, whereas

our previous work has shown great promise of using additive friction stir deposition for underwater and large component repair. For future research in cold spray, strategies are needed to eliminate porosity and improve the as-repaired mechanical properties, especially when depositing high strength-to-weight ratio materials. For additive friction stir deposition, we hope to improve the spatial resolution and portability, possibly by downscaling, and to enable robust repair of high-temperature, high-strength materials.

1. Introduction

Each year, the ever-increasing global production of metal components costs more energy and consumes more materials, causing environmental pollution and overloading through the depletion of non-renewable resources[1-4]. Let us consider raw material production of the most prevalent structural metals: steel and aluminum. The minimum energy cost for refining a single kilogram of iron ore is 8.6 MJ[5], for which 2.63 kg of coal needs to be burned; the energy cost for refining 1 kg aluminum ore is even higher, 21.6 MJ[6], which is equivalent to 6.59 kg of coal consumption[7]. This does not take into account the subsequent hot rolling, forming, fabrication, and transportation steps, for which the energy cost per weight can be comparable to raw material production. In addition to such high embodied energy, metal components are characterized by their massive production. As these two aspects are combined, the overall energy used to produce metal components per year is immense. For steel production alone, the annual energy consumption is equal to ~7% of the total world energy use[8].

To deal with greenhouse gas emissions and climate change, the circular economy model highlights a closed-loop system involving repair, remanufacturing, and recycling of materials[9, 10]. Repair of a damaged metal component, if successful, offers the most direct route to lowering the energy costs, greenhouse gas emissions, and material waste. Beyond energy and environmental

reasons, repair is also the solution when replacement is not economically viable, e.g., when the component is no longer manufactured. The notion of repair can be broad; here, we focus on structural repair, which is defined by two key elements: restoring the original geometry and enabling good mechanical performance in post-repair service. Structural repair has widespread applications in aerospace, automotive, infrastructure, and defense sectors, wherein components can undergo significant wear, thermal fatigue, erosion, corrosion, or chemical reactions.

Depending on the bonding mechanisms and additive capabilities, structural repair technologies can be organized into four categories as shown in Figure 1: non-additive, non-melting-based (Quadrant 1), non-additive, melting-based (Quadrant 2), additive, non-melting-based (Quadrant 3), and additive, melting-based (Quadrant 4). Quadrant 2 denotes the traditional fusion welding approaches, including gas metal arc welding (GMAW), gas tungsten arc welding (GTAW), laser welding, induction welding, etc. Fusion welding uses thermal energy to melt the materials and form metallurgical bonds during co-solidification[11] and has been historically used for most repair geometries. Quadrant 4 is comprised of fusion-based additive manufacturing processes, especially those belonging to directed energy deposition, which enable high geometric precision. Notable examples include laser engineered net shaping (LENS) and wire arc additive manufacturing (WAAM). For structural repair purposes, the fusion-based repair approaches in Quadrant 2 and Quadrant 4 can easily meet the geometry restoration requirement; enabling good mechanical performance (e.g., static and fatigue properties), however, is remarkably challenging due to the underlying liquid phase bonding mechanism. The co-melting and solidification nature inevitably leads to critical issues affecting the post-repair mechanical performance[12, 13], such as solidification porosity, residual stress, hot cracking, stress corrosion cracking, dendritic microstructure formation, and elemental segregation[14].

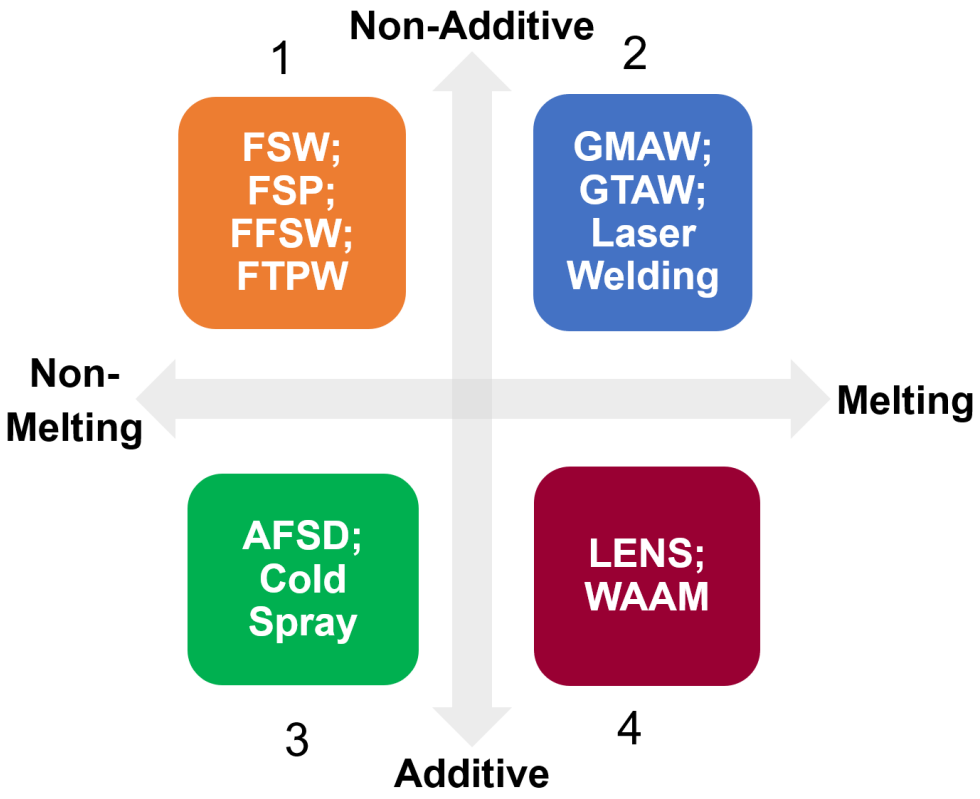

Manuscript 1. Figure 1. Structural repair technologies divided into four quadrants. Quadrant 1: non-additive, non-melting-based, including friction stir welding (FSW), friction stir processing (FSP), filling friction stir welding (FFSW), and friction taper plug welding (FTPW). Quadrant 2: non-additive, melting-based, including gas metal arc welding (GMAW), gas tungsten arc welding (GTAW), and laser welding. Quadrant 3: additive, non-melting-based, including additive friction stir deposition (AFSD) and cold spray. Quadrant 4: additive, melting-based, including laser engineered net shaping (LENS) and wire arc additive manufacturing (WAAM).

The critical issues inherent to fusion-based repair may be addressed or mitigated by turning to solid-state processes. Quadrant 1 in Figure 1 includes solid-state repair approaches without additive capabilities. Within this category, friction stir welding (FSW) and friction stir processing (FSP) ensure good bonding via extensive material flow but are limited to surface and crack repair because filler materials are not used[15]. More recently developed technologies, such as filling friction stir welding (FFSW)[16] and friction taper plug welding (FTPW)[17], can repair volumetric damages. Additionally, the issue with FSW leaving a keyhole has been addressed via methods

such as refill friction spot welding, which can fill the cavity with new material[18]. However, these technologies require the addition of a pre-fabricated piece that must be designed and machined to match the damaged section. To enable structural repair for a wide range of geometries with continuous material feeding, an additive manufacturing capability needs to be incorporated into the solid-state processes—which is Quadrant 3 in Figure 1.

In this Account, we discuss the promise of solid-state metal additive manufacturing-enabled structural repair with a focus on two technologies, cold spray[19] and additive friction stir deposition (AFSD)[20]. We start with a brief review of the fusion-based repair approaches, based on which the needs of solid-state structural repair are highlighted. This is followed by the process specifics of cold spray and AFSD, both of which allow for location-specific material addition via deformation bonding. The repair capabilities of these solid-state processes are evaluated on several metrics, including structural integrity, material choice, geometric compliance, type of repair, and portability. We conclude by emphasizing the importance of further refining the two processes for broader repair applications, as well as recommending several future research directions.

2. Structural Repair by Fusion Welding and Fusion-Based Additive Manufacturing

Fusion-based welding and additive manufacturing are capable of repairing a broad range of geometries, including (i) surface layering or shallow divot repair (Figure 2(a)), (ii) volumetric fill of deep features (Figure 2(b)), (iii) feature reconstruction (Figure 2(c)), and (iv) crack repair (Figure 2(d)). Surface layering denotes the addition of a thin layer on a damaged component after machining away damaged or corroded material. Volumetric fill refers to major material addition to fill in holes, trenches, or grooves. Feature reconstruction involves the complete reformation of a major feature in a component. Crack repair aims to remove the surface defects without changing the component majority. Figure 2(e) and (f) exemplify volumetric fill repair and feature

reconstruction enabled by fusion-based additive manufacturing. The latter involves an irregular damage geometry in a titanium turbine blade.

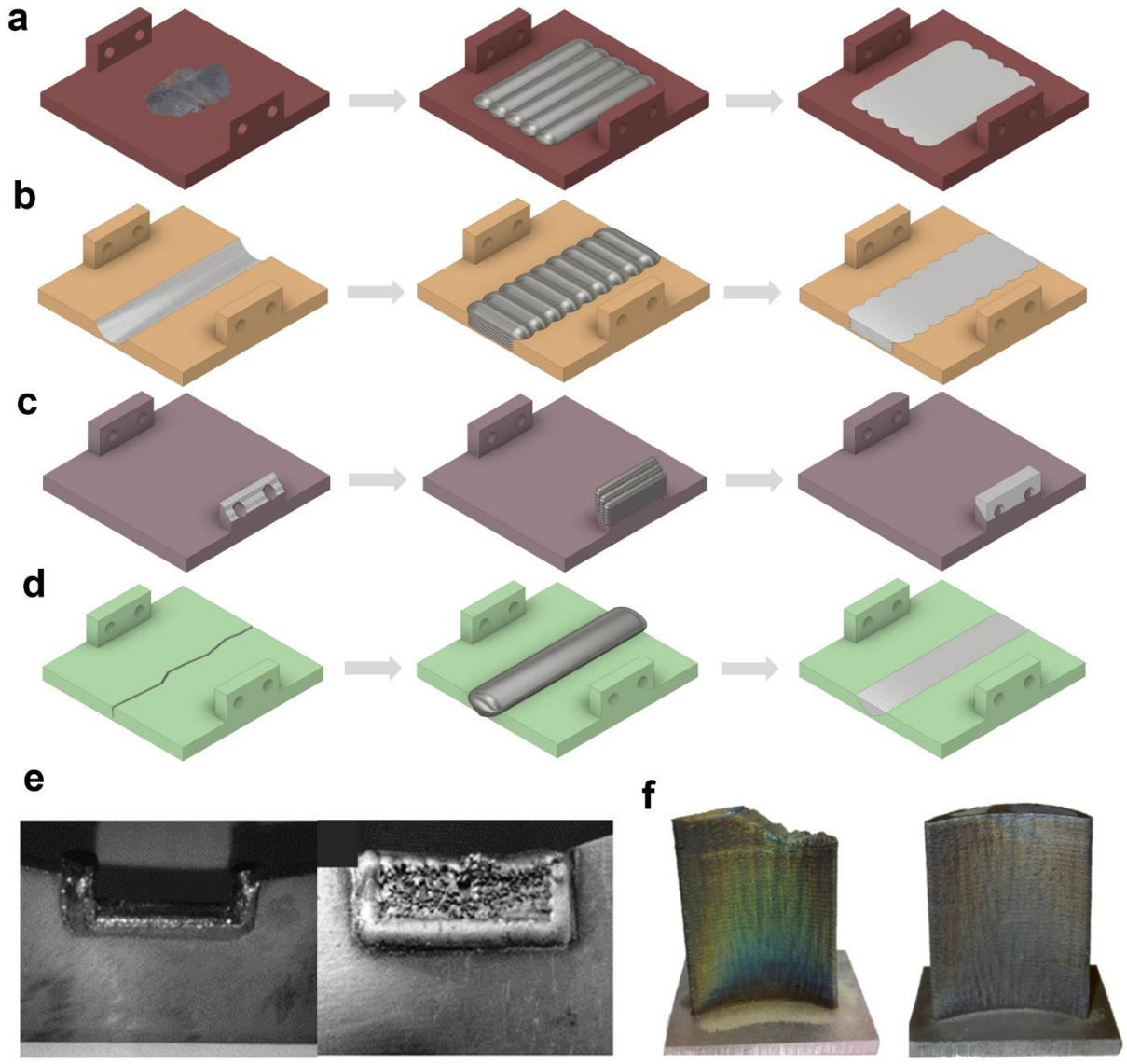

Manuscript 1. Figure 2. Repair geometries enabled by fusion-based approaches. Schematics of (left) original damage, (center) immediately following repair, and (right) surface after final grinding for four types of repairs: (a) surface layering or shallow divot repair, (b) volumetric fill, (c) feature reconstruction, and (d) crack repair. Examples of (e) volumetric fill repair[21] and (f) feature reconstruction[22] by laser metal deposition. (e): reproduced with permission from reference 21. Copyright 2015 Elsevier. (f): reproduced with permission from reference 22. Copyright 2014 Elsevier.

Relying on the same liquid phase bonding mechanism, the main differences between fusion-based welding and additive manufacturing lie in the size of the reaction area, spatial resolution, and hardware specialization. Additive manufacturing technologies generally enable better control of spatial resolution and deposition path, and therefore substantially improve the geometry precision in metal repair[10]. For example, the molten pool size in LENS[14] is typically around 0.25-1 mm wide and 0.1-0.75 mm deep; it is much larger in fusion welding, ~ 3-6 mm wide and 0.7-5.8 mm deep[23]. If fusion welding were used for the blade repair in Figure 2(f), substantial machining would be required to fully restore the original geometry. However, using additive manufacturing, very little post-machining is necessary due to the tight dimensional tolerances, which significantly reduces material waste.

For fusion-based repair approaches, the co-melting and solidification behavior that enables joining and repair is also the largest limitation. Porosity develops when a lack of fusion occurs; when the applied energy is too high, porosity may also develop due to spatter ejection[24]. In addition, various alloys suffer from hot cracking[12, 25, 26] and are deemed "non-weldable". This phenomenon is caused by solidification shrinkage when constituents with low melting temperatures are rejected at the liquid-solid interface, allowing thin liquid areas to form between solidified dendrites. Non-weldable alloys include widely used high-strength aluminum alloys, such as 2xxx and 7xxx series, as well as several more exotic alloys[20, 27, 28]. Moreover, epitaxial solidification results in highly oriented, large columnar grains, which are unfavorable for structural applications due to low strength and mechanical anisotropy.

Often it is desirable to repair with a new, stronger material to extend the component lifetime in a specific damage-prone region. For such dissimilar metal repair, brittle intermetallic phases may form during solidification and promote failure after repair. The large amount of heat

introduced during fusion-based welding and additive manufacturing can also modify the grain structures, change the precipitate attributes, and degrade the mechanical properties in both the repair regions and base metal. This will result in higher susceptibility to damage in future service as compared to the original component. The high thermal gradient across the molten pool and unrepaired region can cause large residual stresses, which are especially severe in fusion-based additive manufacturing owing to the sub-millimeter size of the molten pool and the high cooling rate of approximately $10^3 - 10^5\ K/s$[14]. Finally, extensive use of high energy sources like lasers is contrary to the original intention of repair—to reduce the energy costs and greenhouse gas emissions.

Fundamentally addressing or mitigating the aforementioned issues necessitates the employment of solid-state repair approaches, wherein no melting or solidification is introduced. This motivates us to examine solid-state additive manufacturing approaches for structural repair.

3. Feasible Solid-State Metal Additive Manufacturing Processes for Repair

Within solid-state additive manufacturing, ultrasonic additive manufacturing and friction stir additive manufacturing are precluded because they are sheet lamination-based hybrid processes. To enable the repair of a broad range of geometries like those shown in Figure 2, a freeform process that continuously feeds material and precisely controls the deposition path is preferred. Two candidate processes meet the requirement: cold spray and AFSD.

3.1. The First Candidate: Cold Spray

Figure 3 shows the physical processes and resultant microstructures in cold spray additive manufacturing. Cold spray is similar to spray painting using metal powders rather than paint, wherein a substrate is bombarded with small metal particles of high speed. Upon impact, the particles and substrate co-deform, resulting in interfacial bonding and mechanical interlocking. As

shown in Figure 3(a), the energy needed to create this impact is applied using a high-pressure gas to accelerate small metallic particles to a high velocity, usually over 300 m/s, using a special convergent-divergent de Level nozzle[29, 30]. Upon impact, the particles quickly undergo deformation with a large amount of strain. At sub-critical velocities, such strain hardens the metal and inhibits deformation bonding[31]. However, by increasing the powder velocity above a critical point, the high strain rate allows the surface oxides to be broken up and metal-metal contact to be made at the atomic level.

The metal adhesion in cold spray has long been explained by adiabatic shear instability, based on which the metal softens from adiabatic heating so that jets of material can form at the impact interface[31, 32]. From in situ observations of single micro-particle impact bonding[33], however, Hassani-Gangaraj et al. suggest that adiabatic shear instability may not be the predominant bonding mechanism; instead, the interaction of strong pressure waves with the free surface at the particle edges is sufficient to cause hydrodynamic plasticity and large interfacial strain to enable bonding[34] (see Figure 3(b)). The particle deformation during cold spray is not homogeneous, with more strain localized close to the particle-substrate interface (see Figure 3(c))[35]. With severe deformation, ultrafine grains are often observed at the interfacial region as a result of dynamic recrystallization.

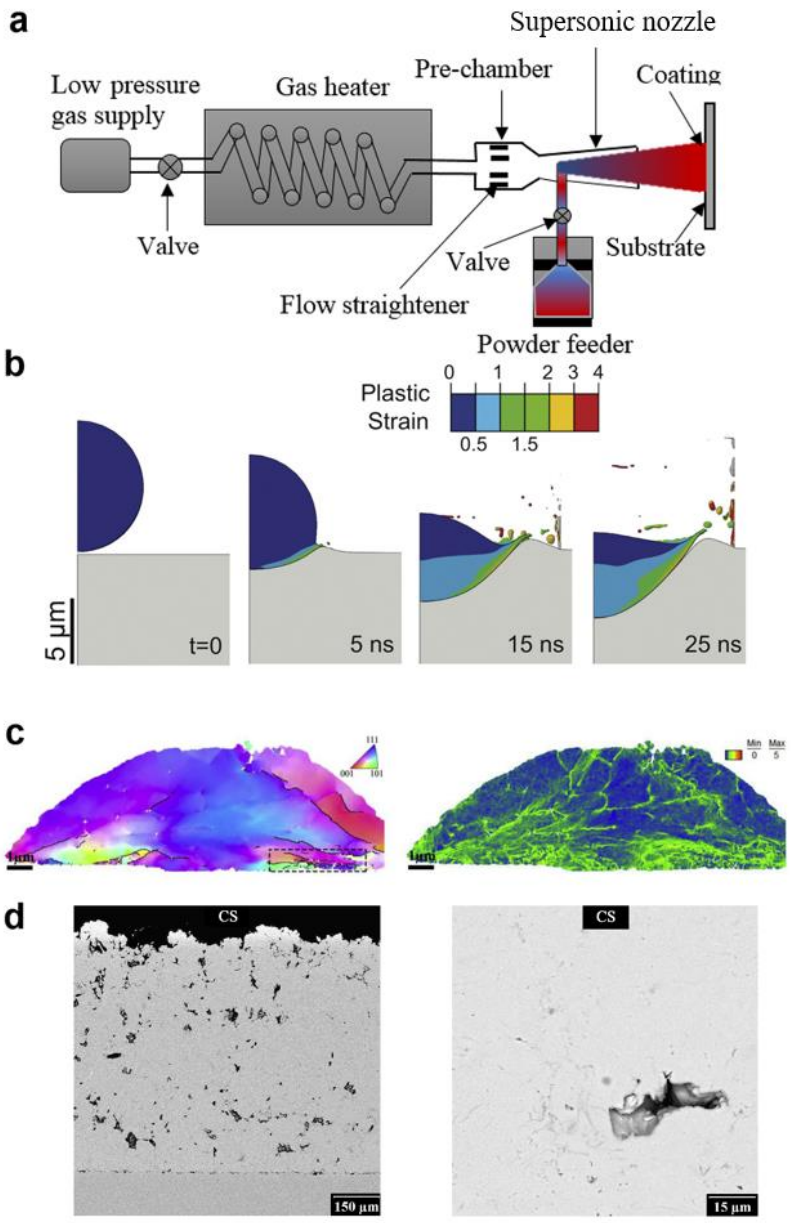

Manuscript 1. Figure 3. Introduction to cold spray. (a) Illustration of the operation principle[36]. (b) Simulation results regarding temporal and spatial evolution of the von Mises plastic strain as a Cu particle impacts a Cu substrate at the critical velocity[34]. (c) (Left) orientation map and (right) kernel average misorientation map of a single Al-2Cu particle deposited onto an AISI 4340 steel substrate at 325°C[35]. (d) The microstructure of cold sprayed Ti-6Al-4V showing porosity and defects at two magnifications[37]. (a): reproduced with permission from reference 36. Copyright 2019 EDP Sciences. (b): reproduced with permission from reference 34. Copyright 2018 Elsevier. (c): reproduced with permission from reference 35. Copyright 2019 Elsevier. (d): reproduced with permission from reference 37. Copyright 2013 Elsevier.

While the powders themselves may be small, usually on the order of tens of microns[38], the larger size of the nozzle dictates the resolution of the resulting deposited material[29]. The more portable low-pressure cold spray system is used for softer metals but is limited to velocities ~ 300-600 m/s. The high-pressure system is better suited for harder metals and is capable of particle velocities ~ 800-1400 m/s[39]. With any given material system, there are multiple parameters under operator control, including the powder feed rate, spray distance, spray angle, scanning step, nozzle traverse speed, gas pressure, gas temperature, and gas type[40], allowing for deposition of various track thicknesses and mechanical properties. As shown in Figure 3(d) for titanium deposition, incomplete mixing, trapped oxides, and porosity are commonly observed in cold spray and can result in inferior as-deposited mechanical properties. Most materials require, or benefit greatly from, preheating to soften the material and enhance deformation.

3.2. The Second Candidate: AFSD

Figure 4 introduces the basic principles and recent fundamental understandings for AFSD. At first glance, AFSD operates analogously to the most common desktop 3D printers using fused deposition modeling. In both processes, material is deposited directly beneath an extrusion assembly. The assembly traverses on a workpiece via multi-dimensional motion to pattern out a layer of deposit. Unlike fused deposition modeling, which simply uses a heating element to melt or plasticize polymers, AFSD leverages friction to rapidly heat up a rotating metallic feed-rod, which reaches an elevated temperature shortly after contacting the non-rotating substrate. With compression from an actuator and torsion caused by the rotating tool, the feed material yields and extrudes below the tool head. Through rapid plastic deformation, additional volumetric heat is generated due to energy dissipation. The deposition principle is illustrated in Figure 4(a).

The extensive material flow and the compression and shear loading states can result in fully-dense as-deposited material, while the co-deformation between the feed material and substrate surface leads to a non-planar interface[41] with strong bonding (Figure 4(b)). The thermal characteristics of AFSD are strongly dependent on the processing parameters, particularly the tool head rotation rate Ω and travel velocity V (Figure 4(c) and (d)). Under normal circumstances, the peak temperature of the material T_{Peak} is between 50% and 90% of its melting point T_M. As shown in Figure 4(e)-(g), the as-deposited material is characterized by significantly refined, equiaxed microstructure due to dynamic microstructural evolution, including continuous and discontinuous dynamic recrystallization. Continuous dynamic recrystallization, which includes geometric dynamic recrystallization and progressive lattice rotation, dominates in AFSD of most aluminum alloys because of their high stacking fault energy. In materials with lower stacking fault energy like copper, discontinuous dynamic recrystallization may play an important role[42]. Because the as-deposited material is fully dense with a fine equiaxed microstructure, the resultant mechanical properties can be comparable to wrought alloys and substantially better than the mechanical properties obtained via fusion-based additive manufacturing[43].

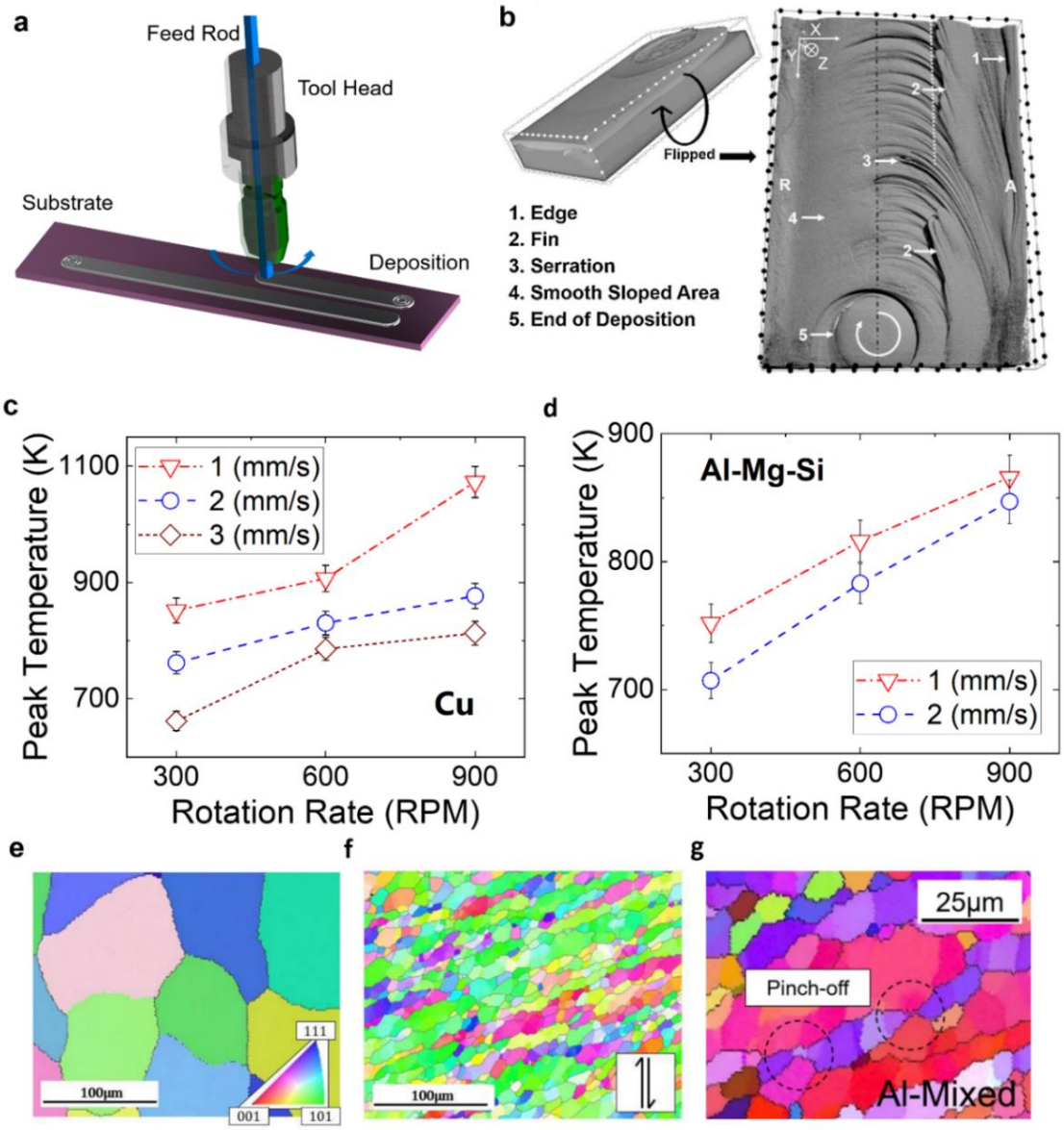

Manuscript 1. Figure 4. Introduction to AFSD. (a) Illustration of the operation principle. (b) Non-planar interface revealed by X-ray computed tomography[41]. Plot of peak temperature as a function of the processing parameters for (c) Cu and (d) Al-Mg-Si[44]. An example of dynamic microstructure evolution in Al-Mg-Si[42], highlighting microstructure refinement from the (e) feed material to (f) as-deposited material with evidence of geometric dynamic recrystallization shown in (g). (b): reproduced with permission from reference 41. Copyright 2020 Elsevier. (c) and (d): reproduced with permission from reference 44. Copyright 2020 Elsevier. (e), (f), and (g): reproduced with permission from reference 42. Copyright 2021 Elsevier.

The standard machines available from MELD Manufacturing Corporation – the leading commercial supplier of AFSD machinery – use 3/8-inch square rod stock as the feed material.

From an environmental standpoint, the use of solid rods and bars as feed material is an understated advantage; the embodied energy for producing a bar is significantly lower than that for drawing a wire or gas-atomizing a powder[45]. For most metals, the machine operates at a rotational rate of 100-1000 RPM and a travel velocity of 1-5 mm/s[44]. In addition to these parameters, the layer height, geometry of tool head, and rate of material feeding are commonly adjusted as well. Following similar material deformation and bonding principles, a technique termed hybrid metal extrusion and bonding has just recently been developed. It uses metal wire fed through an auger as the feed material, which allows for smaller deposition tracks while requiring less power to operate[46].

3.3. A Brief Comparison of the Two Candidate Processes

While both are characterized by large plastic deformation, there is a salient difference in the time scale of the deformation and heating between cold spray and AFSD. In cold spray, strain events are on the time scale of hundreds of nanoseconds and the strain rate is extremely high, up to 10^9/s. In AFSD, the deposited material can spend 10^0-10^1 seconds beneath the tool head at elevated temperatures[44], and the deformation period is likely on the order of tenths of seconds. These time scales are orders of magnitude higher than cold spray. Moreover, there is a wide area surrounding the tool head that experiences secondary heating, and the entire substrate can be heat-soaked depending on conditions—allowing it to reach steady-state conditions much easier.

Figure 5 compares the microstructure evolution of copper deposited via cold spray and AFSD. In both cases, the feed materials, either powder (Figure 5(a)) or solid bar (Figure 5(c)), experience large strain at elevated temperatures, which can result in continuous and discontinuous dynamic recrystallization. With more time and energy for restoration processes to occur, AFSD leads to larger grain sizes, more recrystallization, and less stored energy than cold spray. As a

result, the copper deposited by cold spray (Figure 5(b)) contains a significant portion of submicron grains, whereas the as-deposited copper by AFSD exhibits a grain size ~ tens of microns (Figure 5(d)). The former is also characterized by a substantially higher dislocation concentration and orientation gradient than the latter.

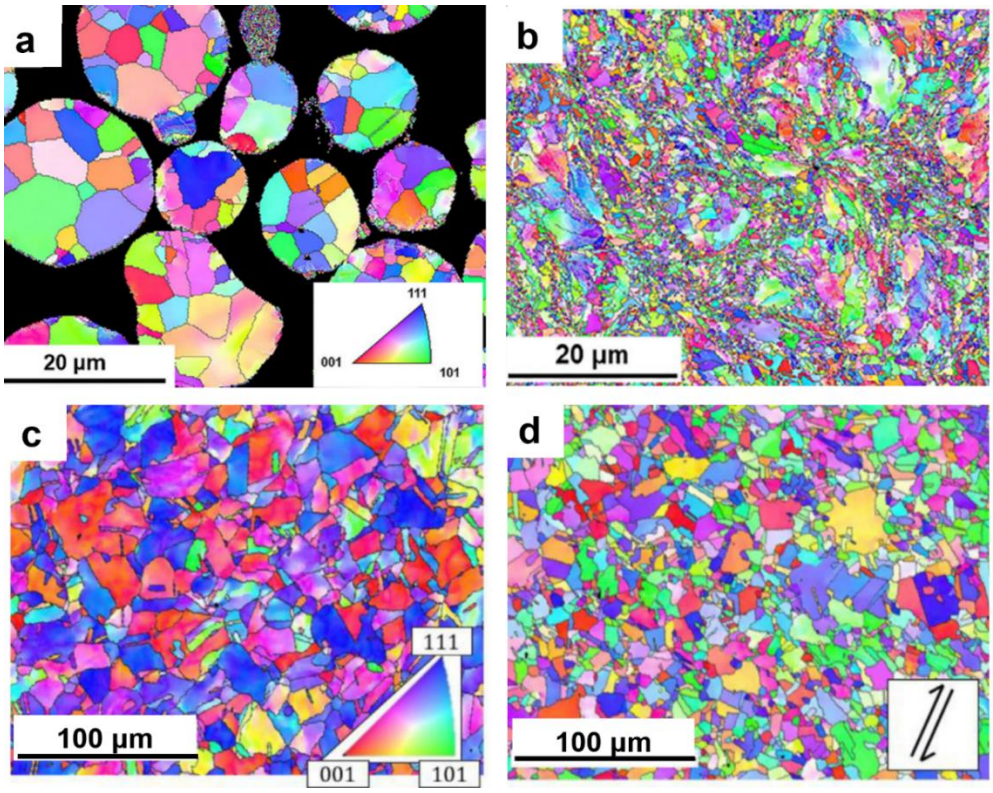

Manuscript 1. Figure 5. A comparison of the Cu microstructures by solid-state additive manufacturing. Cold spray: microstructure of (a) the powder before spray and (b) spray deposition[47]. AFSD: microstructure of (c) the stock rod and (d) as-deposited material[42]. (a) and (b): reproduced with permission from reference 47. Copyright 2020 Elsevier. (c) and (d): reproduced with permission from reference 42. Copyright 2021 Elsevier.

To conclude this section, we compare the key features and working principles of cold spray, AFSD, and fusion-based repair in Table 1, highlighting their advantages and disadvantages.

Manuscript 1. Table 1. Key features, advantages, and disadvantages of cold spray, AFSD, and fusion repair.

	Operating Principle	Build Size/Rate	Advantages	Challenges
Cold Spray	• Deformation-based • Uses powder feed	• Can have large build size if portable • Slower build rate	• Portable • Non-melting	• Low ductility
AFSD	• Deformation-based • Uses bar stock feed	• Print size not limited by machine • Fast build rate	• Fully Dense • Large Parts	• Difficulty with hard metals • Coarse deposition
Fusion Repair	• Melt-based • Uses powder or wire feed	• Small size limited by machine • Fast build rate	• Fine geometric control	• Weldable alloys only

4. Evaluation of Repair Capabilities Based on Key Metrics

Both cold spray and AFSD allow for location-specific material addition and buildup, so they apply to the four types of repair geometries discussed earlier. Instead of melting and solidification, material bonding in repair is implemented by co-deforming a feed material and a substrate, a side wall, or a previous layer. Therefore, there are no concerns of solidification porosity, formation of dendritic microstructure, or hot cracking[48]. These approaches, in theory, have a lot of potential for restoring the original geometry of metal components while retaining good mechanical performance after repair. In this section, we critically assess their repair capabilities based on several key metrics.

4.1. End-Part Structural Integrity

A vital aspect of metal repair is structural integrity, which is perhaps the most compelling reason to choose solid-state additive manufacturing. Producing a repaired section with properties at or near that of the parent material allows for a well-balanced component without potential stress concentrations. Figure 6 compiles stress-strain curves for materials printed by AFSD and cold spray. AFSD excels in this category because, due to the compression and shear imposed by the tool head and the widespread material flow, it can deliver completely dense material in the as-

repaired state. Additionally, the high strain rate deposition of these processes is capable of removing or breaking up surface contamination to enable a strong interfacial bond. The fine, equiaxed microstructures resulting from dynamic recrystallization and the wrought-like mechanical properties are challenging to achieve in fusion-based repair approaches.

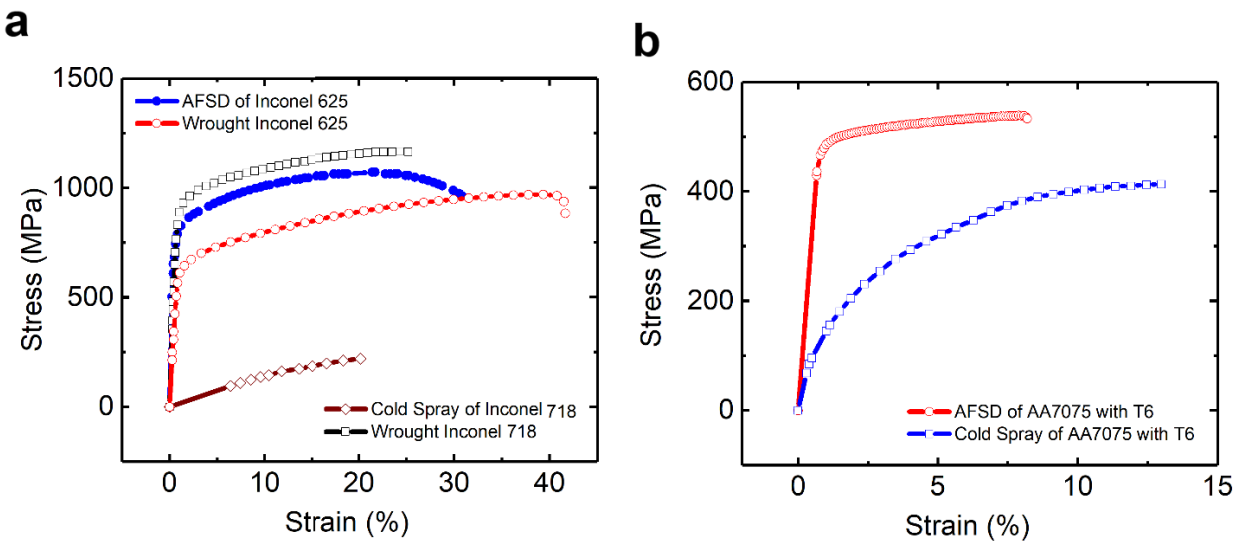

Manuscript 1. Figure 6. Comparison of the stress-strain curves by solid-state additive manufacturing. (a) Inconel 625 alloy by AFSD[49] vs. wrought Inconel 625[50]; Inconel 617 by cold spray[51] vs. wrought Inconel 617[52]. (b) AA7075 by AFSD[48] vs. AA7075 by cold spray[53], both under T6 temper condition. (a): reproduced with permission from reference 49 Copyright 2017 Elsevier; reference 50, Copyright 2019 MDPI; reference 51, Copyright 2013 Springer Nature. (b): reproduced with permission from reference 48, Copyright 2021 Elsevier; reference 53, Copyright 2017 Elsevier.

Figure 6(a) shows that the yield strength of as-deposited Inconel 625 by AFSD[49] is higher than typical wrought Inconel 625[50], while the elongation to failure is slightly decreased. This can be attributed to the significant grain size reduction during dynamic recrystallization in AFSD. Cold spray may result in significantly weaker Inconel 617 depositions due to the imperfect bonding and porosity in the as-deposited state[51]. Post-deposition annealing is generally required to remove the porosity and improve the ductility. Figure 6(b) compares the AA7075 deposited by AFSD and cold spray after T6 condition. The former is able to reach 94% of the wrought yield strength, 95%

of the wrought ultimate tensile strength, and 78% of the wrought elongation by proper solution treatment and aging [48]. While the latter exhibits better elongation, the strength is quite low. It is also important to point out that the as-deposited AA7075 without annealing shows poor ductility[53].

4.2. Portability

It is important to consider the portability of each process; for structural applications, a component often needs to be repaired on site or in use. In its current state, cold spray is significantly more portable than AFSD due to its simplicity in design and lack of high forces required during deposition. Low-pressure cold spray systems are especially portable and can be as simple as an assembly consisting of a tank of compressed air, a pre-heater, a hand-held nozzle, and a gravity-fed powder hopper[54]. AFSD requires a gantry for accurate and rigid positioning of the tool head, wherein the forces applied by the system are balanced out by bracing. It also requires direct power input as opposed to the portable energy derived from compressed gas in cold spray. Since the current AFSD systems are large and heavy, repair of remote or non-grounded sites may be particularly difficult. However, given the successful implementation of portable friction stir welding machines, it is possible that a down-scaled portable AFSD machine could be developed in the future[55].

4.3. Available Materials

For cold spray, in theory, any ductile alloy capable of plastically deforming upon impact can be processed. So far, mainly softer metals, such as copper and aluminum, are repaired using this method due to their lower yield strengths, which allow the kinetic impact to deform metal powders at relatively low velocities[29]. Stronger metals such as steel and titanium can be sprayed, but they tend to lack good ductility or high strength due to the lower amount of mechanical interlocking as well as the presence of pores or other defects. For AFSD, porosity is generally not

an issue thanks to the extensive material flow no matter if the material is soft or hard. Of course, depositing softer materials like copper, aluminum, and magnesium is significantly easier[44] than high-strength materials like titanium, steel, and nickel superalloys[49]. The deposition of high-strength materials requires specialized high-temperature tooling, e.g., based on WC, W-La_2O_3, W-Re, or PCBN (polycrystalline cubic boron nitride)[56]. Wear degradation, catastrophic failure, and higher cost of the tools have significantly limited the widespread use of AFSD for high-strength metal repair.

4.4. Repairable Geometries

Both cold spray and AFSD can be used to repair a wide range of geometries, like those shown in Figure 2. Figure 7 shows a few examples of successful corrosion repair via cold spray and hole/groove-filling via AFSD. Cold spray is uniquely suited for the repair of thin geometries due to the lower forces and has been mainly used for surface damage repair. Figure 7(a)-(d) shows an example of repairing corrosion damage on an aluminum component in a utility engine, which involves cold spray deposition, machining, and surface finishing[19]. For the repair of volumetric damages, flat or rounded geometries are preferred because the surface needs to be at a shallow angle for adequate bonding.

AFSD is advantageous for repairing thicker parts with deep damages: the forces and heat buildup during deposition result in extensive material flow with macroscopic material mixing across the interface[57, 58]. Figure 7(e) shows how to fill a through-hole (1/4” in diameter) in a 1/4” thick AA7075 plate, in which the traveling tool head drives the plasticized material flowing into the hole. By examining the top side (Figure 7(f)), the bottom side (Figure 7(g)), and the cross-section (Figure 7(h)), this strategy is shown to enable complete hole filling with good bonding between the deposited material and sidewall. Figure 7(i) shows another example of filling a wide

groove. AFSD can also print large-scale complex parts like domes and tubes, allowing for internal overhangs of up to 54 degrees[20]. Using a featureless tool, it is possible to clad on thin automotive sheet metals without local distortion or wrinkling[57].

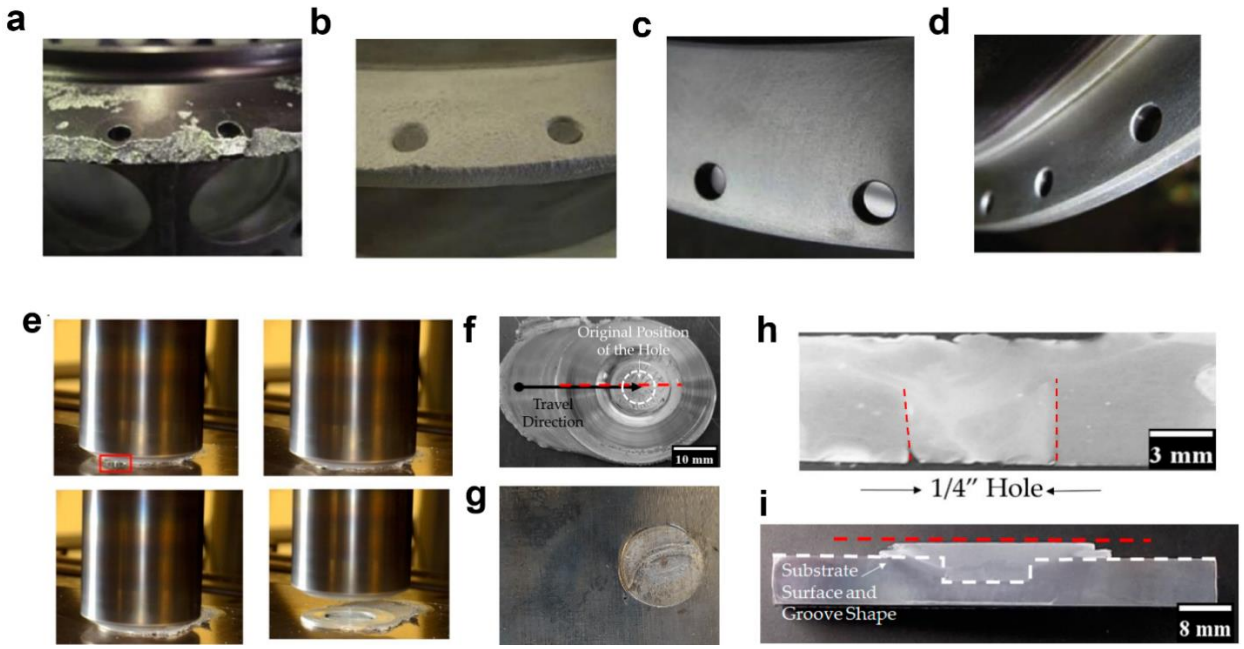

Manuscript 1. Figure 7. Examples of repairable geometries by solid-state additive manufacturing. Cold spray is used to repair corrosion damage: (a) before repair, (b) as-repaired, (c) after machining, (d) after finishing[19]. AFSD is used to fill a through-hole[58]: (e) repair steps, (f) top side, (g) bottom side, and (h) cross-section after repair. (i) Cross-section after filling a wide groove[58]. (a), (b), (c), and (d): reproduced with permission from reference 19. Copyright 2018 Elsevier. (e), (f), (g), (h), and (i): reproduced with permission from reference 58. Copyright 2019 MDPI.

4.5. Geometric Precision

Solid-state metal additive manufacturing does not provide the same level of geometric precision as fusion-based repair approaches. In fusion-based welding and additive manufacturing, small molten pools that allow for high-resolution repair are inherent to the process. The deformation approach of solid-state additive manufacturing results in a much coarser energy distribution, which leads to more material being bonded and a larger size of the minimum obtainable feature. In cold spray, this is seen as a relatively large nozzle diameter when compared

to the width of a laser beam; in AFSD, this is seen as the large size of the tool head channel, which in turn results in an even wider deposition track.

For cold spray, the diameter of the nozzle is 1-3 mm[36] for most material systems. This results in a width of a single track of around 4 mm or more. Note that a single track of material is hill-shaped; to maintain a relatively flat surface, a larger minimum feature size is needed. For a high-pressure system, a characteristic track is around 16 mm wide and 0.35 -2.35 mm thick depending on the traverse speed[29]. For AFSD, the problem with flattened surfaces does not exist as the deposition track has a flat top surface due to the vertical constraint imposed by the tool head. However, the material does spread out during deformation and flow, resulting in a track width of a few centimeters when using a 3/8" feed-rod. With both vertical and side constraints to restrict the material flow, the hybrid metal extrusion and bonding technology has been able to reduce the track width to only 1 cm using a 1.2 mm-wide wire as the feed material[46]. Because of the larger feature size, more post-repair machining is needed in solid-state additive manufacturing-based structural repair, potentially increasing material loss as compared to fusion-based approaches. Scaling down the tooling and instrumentation is a promising research direction for improving geometric precision in these processes.

4.6. Corrosion Resistance

Corrosion is a widespread issue that commonly contributes to the damage of in-service metal components. The solid-state nature of cold spray and AFSD prevents significant oxidation during repair, generally offering improved corrosion resistance as compared to fusion-based repair. For the purpose of structural repair, the repaired component needs to exhibit corrosion resistance better than, or comparable to, the original metal component. In that regard, these two solid-state processes can be applied to dissimilar metal repair, wherein materials that are more chemically

stable against corrosion are deposited to protect the base metal. This strategy has been explored in cold spray research, e.g., deposition of aluminum onto steels[59] and deposition of aluminum on magnesium alloys[60].

For similar metal repair, there are few, if any, published studies directly comparing the corrosion resistance of the deposited material by cold spray and AFSD to the base metal. In principle, the porosity and entrapped oxides in cold spray tend to cause decreased corrosion resistance compared to fully-dense wrought metals. While AFSD can lead to fully-dense deposited materials with wrought-like microstructures, this does not necessarily guarantee improved or comparable corrosion resistance owing to the complex nature of corrosion. The mechanisms for corrosion resistance depend heavily on alloy composition (especially whether the material is active or passive), grain size, dominant grain boundary type, precipitate and second phase behavior, etc.

To conclude this section, we compare the repair capabilities of cold spray, AFSD, and fusion-based repair in Table 2. Clearly, if the as-repaired mechanical performance is the top priority for the target application, AFSD should be selected. If geometric precision is of high priority with minimum post-repair machining preferred, then fusion-based approaches should be considered. If surface damage needs to be fixed and non-weldable alloys are involved, cold spray is the option.

Manuscript 1. Table 2. Comparisons of the repair capabilities among cold spray, AFSD, and fusion approaches.

	End-Part Structural Integrity & Porosity	Portability	Material Choice	Suitable Geometry	Geometric Precision
Cold Spray	Not Fully Dense; Brittle	Excellent	Challenging for Hard Metals	Surface	Coarse
AFSD	Fully Dense; Wrought-like Mechanical Properties	To be Developed	Challenging for Hard Metals	Volumetric	Coarser
Fusion Repair	Not Fully Dense; High Residual Stress	Excellent	Challenging for Non-Weldable Alloys	Both	Fine

5. Niche Repair Applications of Solid-State Metal Additive Manufacturing

5.1. Field Repair of Surface Damages

Mainly caused by corrosion and wear, surface damages are ubiquitous in engineering components, such as turbine blades, engine blocks, landing gears, pistons, and gearboxes[19]. When alloys with poor weldability are involved and when field repair is required, a portable solid-state process like cold spray is the solution. Compared to fusion welding, there is a much lower possibility of forming oxides and brittle intermetallic phases, causing thermal damages to the bulk component, or failing by stress corrosion cracking in post-repair service. Such benefits have been seen in repairing magnesium gear boxes[60] and corroded Al-Mg components in utility engines[61]. Cold spray-based field repair is cost-effective and environmentally acceptable and has been successfully demonstrated in surface protection and dimension restoration for aircraft landing gear[19] (Figure 8(a)).

5.2. Underwater Repair

We next look at the structural repair of critical components in water, such as ship and submarine hulls, propellers, and internal tanks. At present, underwater repair of these components is typically performed using fusion welding. However, mitigation of high residual stress and hot

cracking necessitates the employment of solid-state repair approaches. While friction stir welding has been demonstrated in water, the lack of filler material limits its application to crack repair. AFSD simultaneously addresses the problems associated with melting and continuous material feeding, showing great potential for underwater structural repair with low energy input. Additionally, using an automated process like additive manufacturing reduces the risk of accidents associated with human underwater operation. Recently, our research group has demonstrated underwater cladding and deposition of stainless steel using this process when competing in the American-Made Challenges[62]. Figure 8(b) shows a side view of underwater deposition during AFSD.

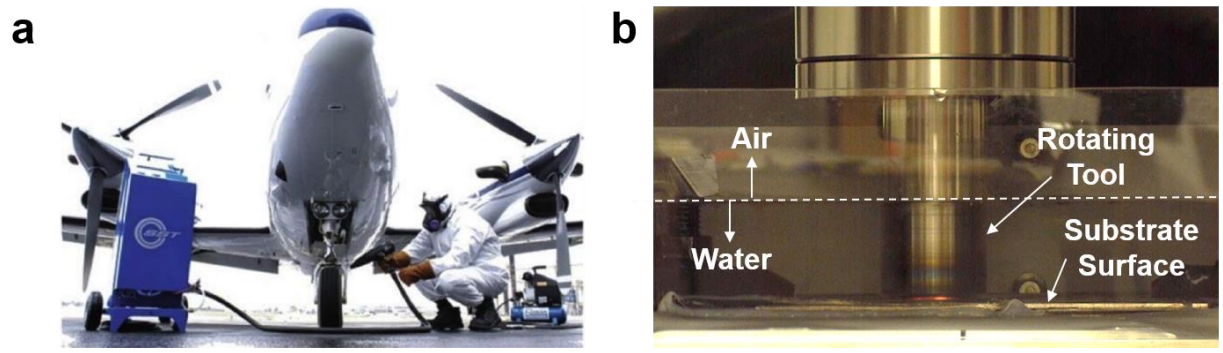

Manuscript 1. Figure 8. Examples of repair applications of solid-state additive manufacturing. (a) Field repair by cold spray[19] and (b) underwater repair by AFSD. (a): reproduced with permission from reference 19. Copyright 2018 Elsevier.

5.3. Large Component Repair

Large components, which can be several cubic meters in volume, have enormous embodied energy, long lead times to produce, and can be extremely difficult to replace. Examples include hydroelectric turbine runners, molding dies, power generator gearbox components, and legacy infrastructures (e.g., I-beams, railways, and various struts, frames, and supports). Fusion-based welding and additive manufacturing can be used to repair them, but likely put substantial residual stress, soften the surrounding material, and accelerate the decay of the component post-repair.

Also, the energy cost for large feature deposition by melting can be remarkably high. Moreover, old infrastructure pieces are often made of a dissimilar alloy than those used in the modern design; such an alloy may be no longer produced and struggle with dissimilar fusion welds.

If caught early, shallow surface damages on these large components can be well repaired by cold spray. If volumetric damages need to be repaired, AFSD can be employed, in which the large tool size and rapid plastic deformation enable a high build rate, on the order of 10^1 pounds/hour for steel and aluminum. This allows for efficient printing of large structures; the buildup of aluminum ring structures with a diameter of 3.05 meters has recently been demonstrated[43]. As a solid-state process, AFSD can repair both weldable and non-weldable materials with lower energy input and thermal gradients. Friction stirring not only results in strong interfacial mixing and bonding, but also can effectively remove the surface dirt, oxides, and corroded materials, possibly reducing the machining efforts. Even when brittle intermetallic phases are formed during dissimilar material deposition, friction stirring likely breaks these phases into globular shapes to mitigate stress concentration.

6. Conclusions and Future Perspectives

Structural repair of metal components is an effective strategy to reduce energy costs and greenhouse gas emissions. However, critical challenges arise using fusion-based repair approaches due to the nature of melting and solidification. Cold spray and AFSD are solid-state metal additive manufacturing processes with great promise for structural repair. These processes enable location-dependent material deposition and can be used for surface damage repair, volumetric filling, feature reconstruction, and crack repair via deformation bonding. Cold spray is highly portable and is best suited for field repair of surface damages; AFSD can lead to excellent mechanical properties in the as-repaired materials and should be employed when structural integrity is a high

priority. Compared to fusion-based repair approaches, the main advantages of cold spray and AFSD are the absence of melting and prevention of high thermal exposure, which are beneficial to avoid hot cracking, oxidation, high residual stress, and weakening of the base metal. The limitations of cold spray and AFSD are mostly associated with their overall coarser deposition features, the challenges in repairing high-strength or high-temperature materials, and less readiness for practical applications given their relatively young ages.

Despite their tremendous potential, we admit that further research is required to fine-tune cold spray and AFSD for widespread structural repair applications. For structural repair by cold spray, the major weakness is associated with inadequate mechanical properties in the as-deposited state caused by porosity, especially in high strength-to-weight ratio materials. An improved understanding of the bonding mechanism may offer new insights into porosity control via tuning the deposition parameters and substrate preheating. For structural repair by AFSD, one promising direction that the authors are looking into is downscaling of the tool and deposition, because many repair geometries require better spatial resolution with narrower deposition tracks. We believe downscaling would also help with portability improvements, for which large deposition sizes and high forces have been the major limiting factors. Additionally, in the current set-up, the temperature during deposition is controlled directly by the rotational rate and the rotational torque. Managing to decouple temperature and deformation via additional heating mechanisms could significantly expand the processing windows to allow various new materials, such as high-strength and high-temperature materials, to be deposited effectively. This would also necessitate the design and manufacturing of robust high-temperature tooling, which is another area of future interest.

Acknowledgment

The authors acknowledge the helpful comments by Dr. David Garcia and Dr. Yunhui Zhu.

HZY acknowledges the support from the DoD MEEP program under award N00014-19-1-2728.

Manuscript 1 References

1. Rahito; Wahab, D. A.; Azman, A. H. Additive Manufacturing for Repair and Restoration in Remanufacturing: An Overview from Object Design and Systems Perspectives. Processes **2019,** 7 (11), 802.

2. World Energy Council. World Energy Resources: 2013 Survey. https://www.worldenergy.org/publications/entry/world-energy-resources-2013-survey (accessed Apr 21, 2021).

3. Patel, D.; Kellici, S.; Saha, B. Green Process Engineering as the Key to Future Processes. Processes **2014,** 2 (1), 311-332.

4. Organisation for Economic Co-operation and Development. Material Resources, Productivity and the Environment. https://www.oecd.org/env/waste/material-resources-productivity-and-the-environment-9789264190504-en.htm (accessed Apr 21, 2021).

5. Fruehan, R. J.; Fortini, O.; Paxton, H. W.; Brindle, R. Theoretical Minimum Energies to Produce Steel for Selected Conditions; Carnegie Mellon University, 2000 https://www.energy.gov/sites/prod/files/2013/11/f4/theoretical_minimum_energies.pdf (accessed Apr 21, 2021).

6. United States Department of Energy. U.S. Energy Requirements for Aluminum Production. https://www1.eere.energy.gov/manufacturing/resources/aluminum/pdfs/al_theoretical.pdf (accessed Apr 21, 2021).

7. United States Department of Energy. How Much Coal, Natural Gas, or Petroleum is Used to Generate a Kilowatthour of Electricicty? https://www.eia.gov/tools/faqs/faq.php?id=667&t=6 (accessed Apr 21, 2021).

8. World Steel Association. Steel Facts 2018. https://www.worldsteel.org/en/dam/jcr:ab8be93e-1d2f-4215-9143-4eba6808bf03/20190207_steelFacts.pdf (accessed Apr 21, 2021).

9. Eurioean Environment Agency. Closing the Loop – An EU Action Plan for the Circular Economy. https://www.eea.europa.eu/policy-documents/com-2015-0614-final (accessed Feb 25, 2021).

10. Leino, M.; Pekkarinen, J.; Soukka, R. The Role of Laser Additive Manufacturing Methods of Metals in Repair, Refurbishment and Remanufacturing – Enabling Circular Economy. Phys. Procedia **2016,** 83, 752-760.

11. Bhadeshia, H.; Honeycombe, R. Chapter 13 - Weld Microstructures. In Steels: Microstructure and Properties (Fourth Edition), Bhadeshia, H.; Honeycombe, R. Eds. Butterworth-Heinemann: 2017; pp 377-400.

12. Jenney, C. L.; O'Brien, A., Welding Handbook, Volume 1 - Welding Science and Technology (9th Edition). American Welding Society (AWS): 2001.

13. Persson, E. L. Aluminum Alloys : Preparation, Properties and Applications. Nova Science Publishers, Incorporated: Hauppauge, UNITED STATES, 2011

14. Gibson, I.; Rosen, D.; Stucker, B. Additive Manufacturing Technologies. Springer: New York, 2015.

15. Mishra, R. S.; De, P. S.; Kumar, N. Introduction. In Friction Stir Welding and Processing: Science and Engineering, Mishra, R. S.; De, P. S.; Kumar, N., Eds. Springer International Publishing: Cham, 2014; pp 1-11.

16. Huang, Y. X.; Han, B.; Tian, Y.; Liu, H. J.; Lv, S. X.; Feng, J. C.; Leng, J. S.; Li, Y. New Technique of Filling Friction Stir Welding. Sci. Technol. Weld. Joining **2011,** 16 (6), 497-501.

17. Cui, L.; Yang, X.; Wang, D.; Hou, X.; Cao, J.; Xu, W. Friction Taper Plug Welding for S355 Steel in Underwater Wet Conditions: Welding performance, microstructures and mechanical properties. Mater. Sci. Eng. **2014,** 611, 15-28.

18. Meng X.; Huang Y.; Cao J.; Shen J.; dos Santos J. F. Recent Progress on Control Strategies for Inherent Issues in Friction Stir Welding. Prog. Mater. Sci. **2021,** 115, 100706.

19. Li, W.; Yang, K.; Yin, S.; Yang, X.; Xu, Y.; Lupoi, R. Solid-State Additive Manufacturing and Repairing by Cold Spraying: A review. J. Mater. Sci. Technol. **2018,** 34 (3), 440-457.

20. Yu, H. Z.; Jones, M. E.; Brady, G. W.; Griffiths, R. J.; Garcia, D.; Rauch, H. A.; Cox, C. D.; Hardwick, N. Non-Beam-Based Metal Additive Manufacturing Enabled by Additive Friction Stir Deposition. Scr. Mater. **2018,** 153, 122-130.

21. Raju, R.; Duraiselvam, M.; Petley, V.; Verma, S.; Rajendran, R. Microstructural and Mechanical Characterization of Ti6Al4V Refurbished Parts Obtained by Laser Metal Deposition. Mater. Sci. Eng. **2015,** 643, 64-71.

22. Wilson, J. M.; Piya, C.; Shin, Y. C.; Zhao, F.; Ramani, K. Remanufacturing of Turbine Blades by Laser Direct Deposition with its Energy and Environmental Impact Analysis. J. Cleaner Prod. **2014,** 80, 170-178.

23. Aucott, L.; Dong, H.; Mirihanage, W.; Atwood, R.; Kidess, A.; Gao, S.; Wen, S.; Marsden, J.; Feng, S.; Tong, M.; Connolley, T.; Drakopoulos, M.; Kleijn, C. R.; Richardson, I. M.; Browne, D. J.; Mathiesen, R. H.; Atkinson, H. V. Revealing Internal Flow Behaviour in Arc Welding and Additive Manufacturing of Metals. Nat. Commun. **2018,** 9 (1), 1-7.

24. Matthews, M. Metal Vapor Micro-Jet Controls Material Redistribution in Laser Powder Bed Fusion Additive Manufacturing. Sci. Rep. **2017,** 7, 4085.

25. Phillips, D. H., Welding Engineering - An Introduction. John Wiley & Sons: 2016.

26. O'Brien, A.; Sinnes, K. Welding Handbook, Volume 5 - Materials and Applications, Part 2. 9 ed.; American Welding Society: 2015.

27. Martin, J. H.; Yahata, B. D.; Hundley, J. M.; Mayer, J. A.; Schaedler, T. A.; Pollock, T. M. 3D Printing of High-Strength Aluminium Alloys. Nature **2017,** 549 (7672), 365-369.

28. Mishra, R. S.; De, P. S.; Kumar, N. Friction Stir Welding of Magnesium Alloys. In Friction Stir Welding and Processing: Science and Engineering, Mishra, R. S.; De, P. S.; Kumar, N., Eds. Springer International Publishing: Cham, 2014; pp 149-187.

29. Yin, S.; Cavaliere, P.; Aldwell, B.; Jenkins, R.; Liao, H.; Li, W.; Lupoi, R. Cold Spray Additive Manufacturing and Repair: Fundamentals and Applications. Addit. Manuf. **2018,** 21, 628-650.

30. Tiamiyu, A. A.; Schuh, C. A. Particle Flattening During Cold Spray: Mechanistic Regimes Revealed by Single Particle Impact Tests. Surf. Coat. Technol. **2020,** 403, 126386.

31. Assadi, H.; Gärtner, F.; Stoltenhoff, T.; Kreye, H. Bonding Mechanism in Cold Gas Spraying. Acta Mater. **2003,** 51 (15), 4379-4394.

32. Grujicic, M.; Zhao, C. L.; DeRosset, W. S.; Helfritch, D. Adiabatic Shear Instability Based Mechanism for Particles/Substrate Bonding in the Cold-Gas Dynamic-Spray Process. Mater. Des. **2004,** 25 (8), 681-688.

33. Hassani-Gangaraj, M.; Veysset, D.; Nelson, K. A.; Schuh, C. A. In-situ Observations of Single Micro-Particle Impact Bonding. Scr. Mater. **2018,** 145, 9-13.

34. Hassani-Gangaraj, M.; Veysset, D.; Champagne, V. K.; Nelson, K. A.; Schuh, C. A. Adiabatic Shear Instability is Not Necessary for Adhesion in Cold Spray. Acta Mater. **2018,** 158, 430-439.

35. Liu, T.; Leazer, J. D.; Brewer, L. N. Particle Deformation and Microstructure Evolution During Cold Spray of Individual Al-Cu Alloy Powder Particles. Acta Mater. **2019,** 168, 13-23.

36. Oyinbo, S. T.; Jen, T.-C. A Comparative Review on Cold Gas Dynamic Spraying Processes and Technologies. Manuf. Rev. **2019,** 6, 25.

37. Cizek, J.; Kovarik, O.; Siegl, J.; Khor, K. A.; Dlouhy, I. Influence of Plasma and Cold Spray Deposited Ti Layers on High-Cycle Fatigue Properties of Ti6Al4V Substrates. Surf. Coat. Technol. **2013,** 217, 23-33.

38. Dowding, I.; Hassani, M.; Sun, Y.; Veysset, D.; Nelson, K. A.; Schuh, C. A. Particle Size Effects in Metallic Microparticle Impact-Bonding. Acta Mater. **2020,** 194, 40-48.

39. Moridi, A.; Hassani-Gangaraj, S. M.; Guagliano, M.; Dao, M. Cold Spray Coating: Review of Material Systems and Future Perspectives. Surf. Eng. **2014,** 30 (6), 369-395.

40. Glass, S. W.; Larche, M. R.; Prowant, M. S.; Suter, J. D.; Lareau, J. P.; Jiang, X.; Ross, K. A. Cold Spray NDE for Porosity and Other Process Anomalies. AIP Conference Proceedings 2018, 1949 (1), 020010. DOI: https://doi-org.ezproxy.lib.vt.edu/10.1063/1.5031507

41. Perry, M. E. J.; Griffiths, R. J.; Garcia, D.; Sietins, J. M.; Zhu, Y.; Yu, H. Z. Morphological and Microstructural Investigation of the Non-Planar Interface Formed in Solid-State Metal Additive Manufacturing by Additive Friction Stir Deposition. Addit. Manuf. **2020,** 35, 101293.

42. Griffiths, R. J.; Garcia, D.; Song, J.; Vasudevan, V. K.; Steiner, M. A.; Cai, W.; Yu, H. Z. Solid-State Additive Manufacturing of Aluminum and Copper Using Additive Friction Stir Deposition: Process-Microstructure Linkages. Materialia **2021,** 15, 100967.

43. Yu, H. Z.; Mishra, R. S. Additive Friction Stir Deposition: a Deformation Processing Route to Metal Additive Manufacturing. Mater. Res. Lett. **2021,** 9 (2), 71-83.

44. Garcia, D.; Hartley, W. D.; Rauch, H. A.; Griffiths, R. J.; Wang, R.; Kong, Z. J.; Zhu, Y.; Yu, H. Z. In situ Investigation Into Temperature Evolution and Heat Generation During Additive Friction Stir Deposition: A Comparative Study of Cu and Al-Mg-Si. Addit. Manuf. **2020,** 34, 101386.

45. Digital Alloys. Energy Consumption in Metal Additive Manufacturing. https://www.digitalalloys.com/blog/energy-consumption-metal-additive-manufacturing/ (accessed Apr 4, 2021).

46. Blindheim, J.; Grong, Ø.; Aakenes, U. R.; Welo, T.; Steinert, M. Hybrid Metal Extrusion & Bonding (HYB) - a New Technology for Solid-State Additive Manufacturing of Aluminium Components. Procedia Manufacturing **2018,** 26, 782-789.

47. Liu, Z.; Wang, H.; Haché, M. J. R.; Chu, X.; Irissou, E.; Zou, Y. Prediction of Heterogeneous Microstructural Evolution in Cold Sprayed Copper Coatings Using Local Zener-Hollomon Parameter and Strain. Acta Mater. **2020,** 193, 191-201.

48. Yoder, J. K.; Griffiths, R. J.; Yu, H. Z. Deformation-Based Additive Manufacturing of 7075 Aluminum With Wrought-Like Mechanical Properties. Mater. Des. **2021,** 198, 109288.

49. Rivera, O. G.; Allison, P. G.; Jordon, J. B.; Rodriguez, O. L.; Brewer, L. N.; McClelland, Z.; Whittington, W. R.; Francis, D.; Su, J.; Martens, R. L.; Hardwick, N. Microstructures and Mechanical Behavior of Inconel 625 Fabricated by Solid-State Additive Manufacturing. Mater. Sci. Eng. **2017,** 694, 1-9.

50. de Oliveira, M.M.; Couto, A.A.; Almeida, G. F.C.; Reis, D.A.P.; de Lima, N.B.; Baldan, R. Mechanical Behavior of Inconel 625 at Elevated Temperatures. Metals **2019**, 9(3), 301.

51. Wong, W.; Irissou, E.; Vo, P.; Sone, M.; Bernier, F.; Legoux, J. G.; Fukanuma, H.; Yue, S. Cold Spray Forming of Inconel 617. J. Therm. Spray Technol. **2013,** 22 (2), 413-421.

52. Unocic, K.A.; Kolbus, L.M.; Dehoff, R.R.; Dryepondt, S.N.; Pint, B.A. High-temperature Performance of UNS N07718 Processed by Additive Manufacturing. http://www.osti.gov/scitech/biblio/1132980 (accessed Apr 12, 2021).

53. Rokni, M. R.; Widener, C. A.; Champagne, V. K.; Crawford, G. A.; Nutt, S. R. The Effects of Heat Treatment on 7075 Al Cold Spray Deposits. Surf. Coat. Technol. **2017,** 310, 278-285.

54. Kashirin, A.; Klyuev, O.; Buzdygar, T.; Shkodkin, A. Modern Applications of the Low Pressure Cold Spray. http://en.dymet.net/uploads/fotos/12.pdf (accessed Mar 3, 2021).

55. Rohith Renish, R.; Pranesh, M. A.; Logesh, K. Design and Analysis of a Portable Friction Stir Welding Machine. Mater. Today: Proc. **2018,** 5 (9), 19340-19348.

56. Liu, F. C.; Hovanski, Y.; Miles, M. P.; Sorensen, C. D.; Nelson, T. W. A Review of Friction Stir Welding of Steels: Tool, Material Flow, Microstructure, and Properties. J. Mater. Sci. Technol. **2018,** 34 (1), 39-57.

57. Hartley, W. D.; Garcia, D.; Yoder, J. K.; Poczatek, E.; Forsmark, J. H.; Luckey, S. G.; Dillard, D. A.; Yu, H. Z. Solid-State Cladding on Thin Automotive Sheet Metals Enabled by Additive Friction Stir Deposition. J. Mater. Sci. Technol. **2021,** 291.

58. Griffiths, R. J.; Petersen, D. T.; Garcia, D.; Yu, H. Z. Additive Friction Stir-Enabled Solid-State Additive Manufacturing for the Repair of 7075 Aluminum Alloy. Appl. Sci. **2019,** 9 (17), 3486.

59. da Silva, F.S.; Bedoya, J.; Dosta, S.; Cinca, N..; Cano, I.G.; Guilemany, J.M.; Benedetti, A.V. Corrosion Characteristics of Cold Gas Spray Coatings of Reinforced Aluminum Deposited Onto Carbon Steel. Corros. Sci. **2017,** 114, 57-71.

60. Champagne, V. K. The Repair of Magnesium Rotorcraft Components by Cold Spray. Failure Anal. Prev. **2008,** 8 (2), 164-175.

61. Villafuerte, J.; Wright, D. Practical cold spray success: Repair of Al and Mg Alloy Aircraft Components. Adv. Mater. Processes **2010,** 168 (5), 53-55.

62. Griffiths, R. J.; Perry, M. E. J.; Hartley, W. D.; Garcia, D.; Yu, H. Z. Augmented Repair via Additive Manufacturing 2020. https://www.herox.com/iamhydro/round/656/entry/33593 (accessed Apr 20, 2021).

Chapter 3: Custom Machine Design and Downscaling

Up to this point, much of the work presented has focused on the current state of solid-state additive manufacturing. For AFSD, most of the discussion has focused on its material capabilities while considering its mobility weaknesses. As alluded to in the conclusions of Manuscript 1, a promising direction is to downscale the processes and decouple the heating of the feed material from the rotational speed chosen. To explore the possibility of this endeavor, the following project and experiment were conducted and documented in a letter to be submitted to Additive Manufacturing Letters. The style of this manuscript follows that of the journal.

3.1 Manuscript 2: Transforming a Desktop Mill for Miniaturized Solid-State Metal Additive Manufacturing

Transforming a Desktop Mill for Miniaturized Solid-State Metal Additive Manufacturing

Ryan B. Gottwald, Nikhil Gotawala, Donald J. Erb, Hang Z. Yu *

Department of Materials Science and Engineering, Virginia Tech, Blacksburg, VA 24061, USA.

* Corresponding Author: hangyu@vt.edu

Abstract

Conventional solid-state additive manufacturing enables the repair and fabrication of many previously non-processable materials while retaining the mechanical properties of the feed material. However, the technology historically uses expensive and bulky equipment to enable large deposition tracks. While useful for large-part manufacturing, significant material is wasted when repairing or replacing small components. To overcome this, a low-cost benchtop milling machine was converted into a miniaturized solid-state additive manufacturing setup. This was accomplished

by installing an automatic feed system in place of the milling machine's quill spindle handle enabling downward material feed. A durable and dependable deposition tooling piece was also created and constructed to aid in frictional heating and material flow. We included auxiliary heating to make it easier to deposit high-temperature materials like high-strength steels. To assess deposition and substrate temperatures and the forces applied to the feed on the spot, we fitted the machine with several sensors to enable in-situ monitoring. The overall quality of the deposition is promising and proves that reducing deposition size through this avenue is an attractive option for downscaling the technology.

1. Introduction

Beam-based or fusion-based metal additive manufacturing technologies, such as selective laser melting (SLM), e-beam melting (EBM), and laser engineered net shaping (LENS) [1] excel at creating geometric features out of the desired material, but they are often unable to meet the strength and elongation requirements for their alloy specifications. This results from the challenges rooted in melting and solidification [2], such as porosity, high residual stress, hot cracking, and cast microstructure. To address such issues, non-beam-based, solid-state additive manufacturing technologies are growing at an accelerated rate and are attracting substantial interest from the aerospace and defense sectors recently. Notable examples in this category include cold spray additive manufacturing [3] and additive friction stir deposition [4], both of which leverage severe plastic deformation to implement metallurgical bonding across the printed layers. In these deformation-based additive processes, the feed material, which can be a stream of particles or a solid bar, typically undergoes dynamic recrystallization to result in fine, equiaxed microstructures instead of forming solidification microstructures [5].

Deformation-based metal additive technologies hold great promise for bulk manufacturing and structural repair of high-end components, but they are currently characterized by large feature sizes [6]. For example, the nozzle diameter in cold spray is generally 1-3 mm, resulting in a hill-shaped single-track width of greater than 4 mm. To maintain a flat surface, a larger minimum feature size of greater than 15 mm is often required. Using commercial additive friction stir deposition facilities, the feed-rod has a diameter of approximately 10 mm or larger, and the typical track width of Al deposition is 30-40 mm [7]. Manufacturing or repairing parts with small feature sizes or defects necessitates miniaturization of the nozzle or print head to allow for narrow track widths. Other limitations include the massive footprints and high costs of commercially available machines. As a result, these deformation-based additive technologies have been restricted to industrial use. This is in great contrast to the benchtop milling machines widely available in garage workshops owned by individual families.

Here, we bridge the above gaps by converting an inexpensive desktop milling machine into a small-scale solid-state metal additive manufacturing. By replacing the quill spindle handles in the mill with an automated feed mechanism, downward material feeding is implemented. A reliable tool piece is designed to rotate during deposition and smear the deposited material underneath to promote frictional heating and drive material flow. We introduce auxiliary heating to ease the deposition of high-temperature materials, such as high-strength steels. We also instrument the machine with in situ monitoring capabilities, enabling in situ measurement of the temperature of the deposition and substrate as well as the force imposed onto the feed material. Through these efforts, a standard, low-cost mill has been converted into a simple and convenient facility for solid-state metal additive manufacturing with narrow tracks approximately 10 mm wide

or less. The efficacy of this work is demonstrated by dissimilar material printing using a high-strength martensite steel, AISI 4140, deposited onto a low-carbon steel, AISI 1018.

2. Machine design and instrumentation

Modifications were made to a Precision Matthews PM-728VT bench-type milling machine (cost of $3700) according to **Error! Reference source not found.**1 (A). The mill featured a 1HP motor and was outfitted with a precision ball screw set on the X and Y axes driven by 2.8A Nema 23 stepper motors. This was to enable automatic motion of the substrate along X- and Y- directions. The quill spindle handles were replaced with an automated feeding mechanism driven by a Nema 17 stepper motor with a 5.19 planetary gear reduction. The feed rod with a 3.2 mm × 3.2 mm square cross-section was securely held in a collet in the mill's spindle. The electronics for the mill, which were driven by an ESP32 microcontroller, can be seen in the block diagram in **Error! Reference source not found.**1 (C). The microcontroller processes the positional G-Code commands from a custom python GUI and converts the desired positions into discrete steps to send to the stepper motors. The stepper motors were controlled by commercially available stepper motor drivers (DM542T) through a transistor array to isolate the current flow from the microcontroller pins.

Additionally, a series of machined components were mounted to the mill's side to support the bottom of the feed rod. By turning the spindle handle with the feeding mechanism, the rotating feed rod was pushed through the base of the tool support and into contact with the substrate causing frictional heat. The heat causes material softening; applying pressure through the feeding mechanism then causes yielding and material deposition. Moreover, an induction heater was placed beneath the deposition substrate on the mill bed to enable auxiliary heating of the substrate. Substrates for deposition were affixed to a 4.75 mm-thick steel plate mounted above a 250 W

induction coil. The system had increased rigidity by attaching the substrates to this steel plate. Additionally, ferrous and non-ferrous metals could benefit from auxiliary heating due to the steel backing plate providing the heating. Figure 1(B) shows a picture of the desktop mill after instrumentation.

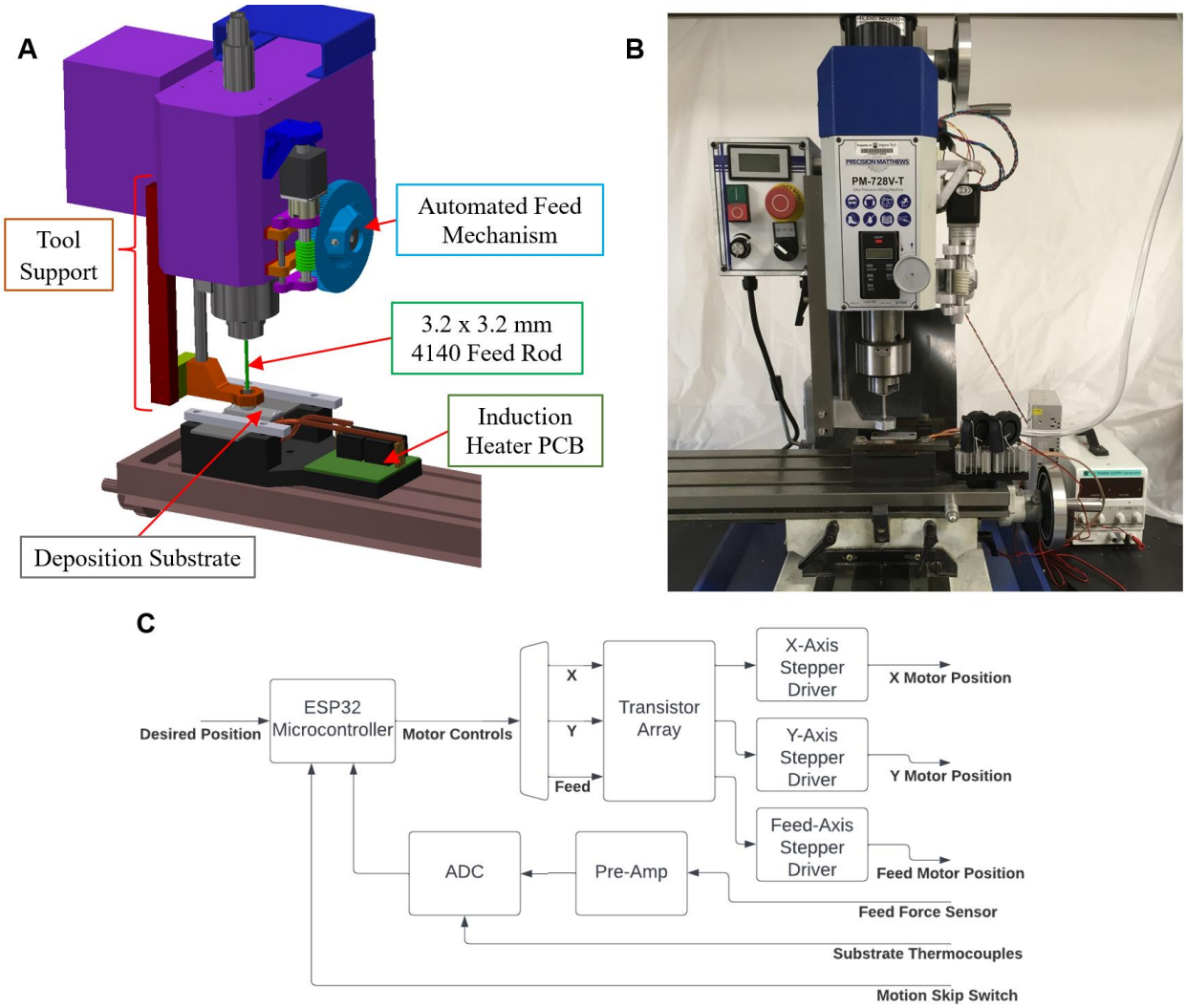

Figure 1. (A) A schematic and (B) a picture of the instrumented desktop mill for miniaturized solid-state metal additive manufacturing. (C) Block diagram of the electrical components of the modified milling machine.

To generate more friction heat and material flow, an innovative tool piece was designed and created as illustrated in detail in Figure 2. Mounted onto the tool support (see Figure 2(A)), this center-hollowed tool piece consisted of a steel holder, a ball bearing structure, and a tungsten

insert (see the dimensions and shapes in Figures 2(B) and 2(C)). In this geometric configuration, the rotation of the feed rod was driven by the mill's spindle, creating frictional heat at the material-substrate interface. The ball bearing structure was used to ensure rotation of the tool piece through torque transfer from the spindle motor, through the collet, into the feed-rod, and finally to the tool. During deposition, the rotating tool piece was in direct contact with the top of the deposition track, imposing compression and shear to plasticize the material further and promote interface mixing. The tool piece needs to remain rigid at the material deposition temperature; deposition of Ti alloys, Ni alloys, and steels would require the employment of expensive W alloys or PCBN (polycrystalline cubic boron nitride). To reduce the tool cost, instead of fabricating a monolithic tool piece using W alloys or PCBN, here we designed an insert structure (5 mm thick) made of a tungsten alloy (25%Re-75%W). This modular part could be easily replaced with a new insert if significant tool wear or damage occurred.

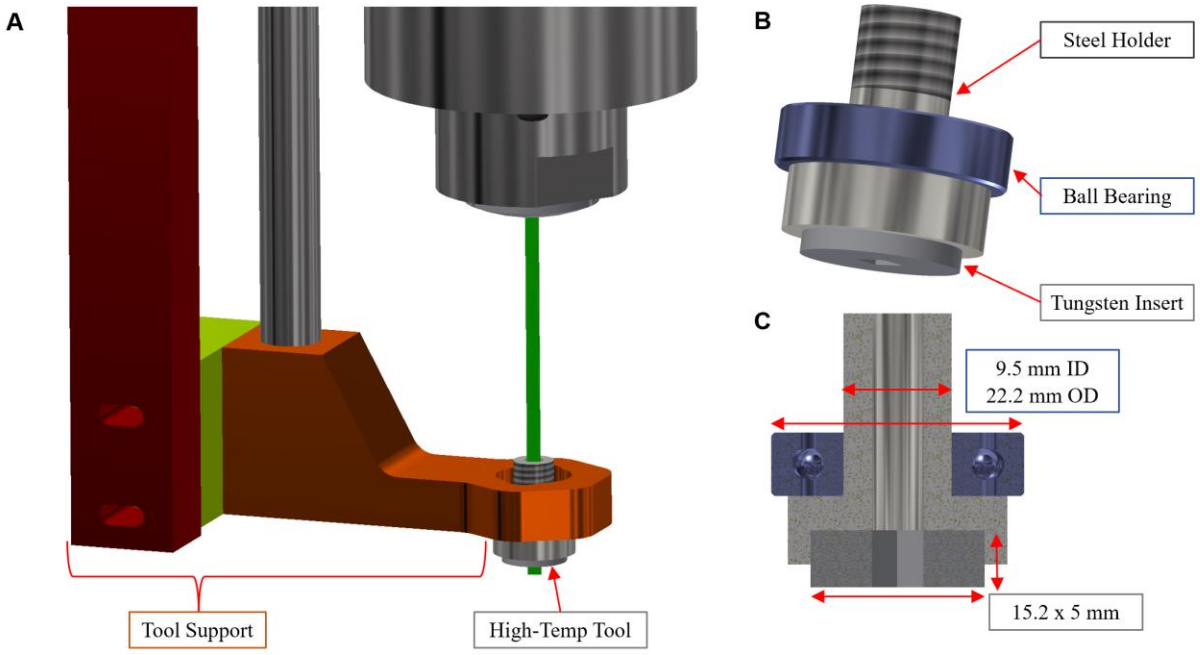

Figure 2. (A) A schematic showing the tool support structure and placement of the designed tool piece. (B) Angle view and (C) cross-section view of the tool pieces, showing geometric details of the steel holder, ball bearing structure, and W alloy insert.

Finally, several sensors were incorporated for in situ monitoring, most of which can also be seen in the electronics block diagram in **Error! Reference source not found.**1 (C). Behind the feeding mechanism's motor was an in-line force sensor capable of measuring the axial pressure applied to the feed material. By incorporating the in-line force measurements into a feedback loop, the feeding rate during the initial heat generation phase could be controlled to maintain a constant downward pressure before yielding the feed material. Additionally, two substrate-mounted thermocouples and a line-skip button were wired into the ESP32 microcontroller. The line-skip button was of great importance as it allowed the machine operator to manually cancel the slow feed rod dwell during heat generation when sufficient heat was built and deposition could occur. The milling machine was also instrumented with thermal imaging and optical cameras. The optical and thermal cameras were mounted as closely as possible to capture similar fields of view. The readings of the thermal camera were calibrated before testing using a thermocouple. This allowed the researchers to account for the view factor of the tool as well as its true emissivity.

3. Material deposition and characterization methods

The instrumented set-up was tested through dissimilar material printing, which involved the deposition of AISI 4140 steel onto a 3.175 mm-thick substrate made of AISI 1018 steel. The key parameters governing the deposition were the target layer height, the revolution speed of the assembly, the traversal speed, and the feeding rate. Preliminary feasibility testing was done to determine the optimal set of machine parameters to allow for proper deposition. For the deposition results presented in this work, the target layer height was 750 μm, the revolution speed was 2500 RPM, the traversal speed was 60 mm/min, and the feeding rate was 40 mm/min. Additionally, the substrate was heated to 230 ℃ before deposition through induction-based auxiliary heating. The feed rod was fed in at an initial rate of 5 mm/min before traversal to build heat.

After deposition, hardness across the interface and the base materials were measured using a Phase II micro-Vickers 900-390 tester with a 9.8 N load and 15-second dwell time. The microstructures of the deposition and substrate were examined using a scanning electron microscope (SEM, FEI Quanta 600 FEG). The crystal structures and grain morphologies were investigated using electron backscattered diffraction (EBSD, FEI Helios 600 NanoLab) after electropolishing the materials.

4. Results

Figure 3 shows the in-situ monitoring results of thermal and mechanical signals during the deposition of a single track of AISI 4140 steel onto an AISI 1018 substrate. The deposition can be divided into two major stages. First, the rotating feed rod is slowly pushed downwards without in-plane traveling. Frictional heat is created at the interface between the feed rod and substrate, resulting in a temperature increase in the feed rod, substrate surface, and tool piece. This is observed in the thermal and optical images from Figure 3 (A) to Figure 3 (C). Next, once sufficient heat has built up, the feeding rate increases, and the tool begins in-plane motion. This further increases the tool's temperature and produces a line of material behind the movement of the tool, as seen in Figure 3 (D).

To get an approximation of the temperature of deposition, the temperature of the outside of the tool was monitored for the duration of the run using the thermal camera. This can be seen in Figure 3 (E). After 45 seconds of heat generation, denoted by point B which corresponds to the time in Figure 3 (B), the external face of the tool began increasing in temperature. This continued up to the beginning of traversal at point C, where the tool was 675 ℃. Once traversal started, the temperature of the tool quickly increased due to the additional heat from the bump in the feed rate from 5 mm/min to 40 mm/min. This caused the tool to settle quickly at its steady-state temperature

of approximately 750 ℃. Finally, a slight cooling can be seen to occur following point D once the deposition had completed and motion ceased.

Looking at the loading during deposition, the force quickly increases 20 seconds after point A. This is due to the small gap between the feed rod and the substrate that took the feed rod 20 seconds to move. After this point, the force quickly climbs to a critical point of 1200 N where the feed rod yields at its heightened temperature. At the onset of deposition, seen in point C, the force drastically increases due to swaging. As the feed rod is pushed faster, it swells inside the tool and forms to the interior shape of the square cutout. This swelling increases the friction on the inner walls, which the feeding mechanism must overcome. Fortunately, the feeding mechanism was capable of supplying the necessary force, and the deposition continued without jamming.

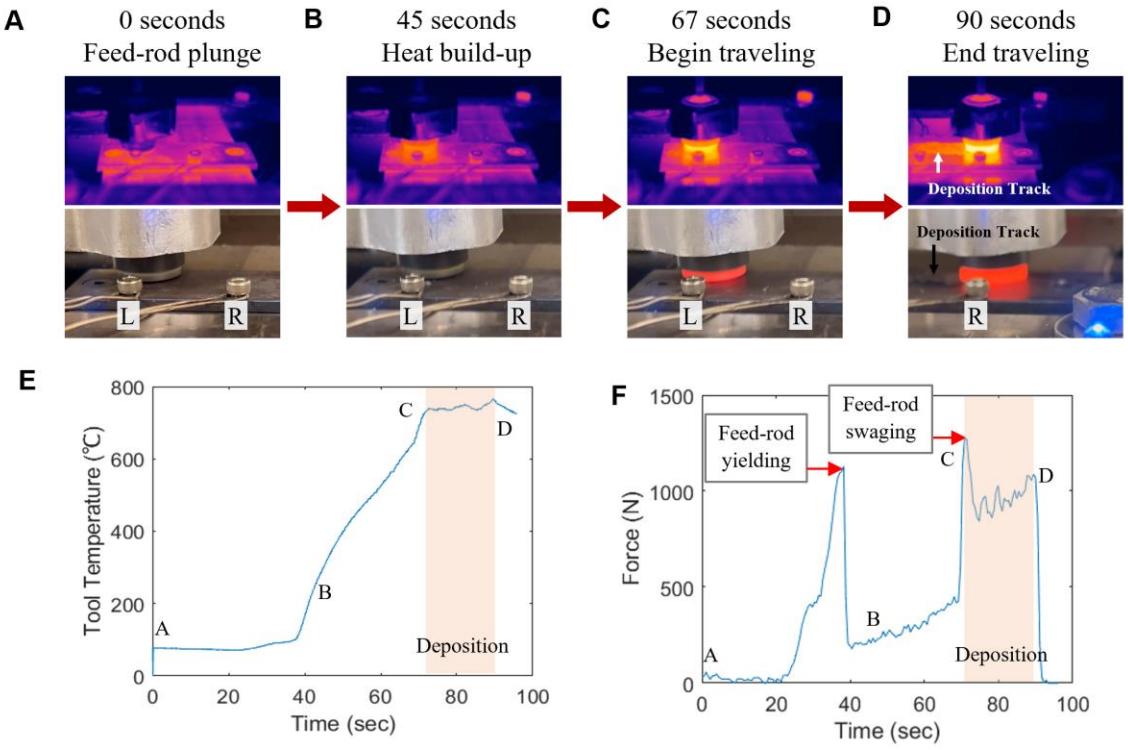

Figure 3. (a) Synchronized thermal (top) and optical (bottom) videos showing the progression of the deposit. (b) Right thermocouple measurements of the substrate 10 mm below the deposition track. (c) A plot of the axial force applied to the square feed rod showing the onset of yielding and swaging.

The completed deposition, which can be seen in Figure 4(A), shows good quality. It is shifted from the centerline of the tool's movement toward the right. Since the tool was rotating clockwise, this suggests that the material was being dragged toward the retreating side during printing [8]. The discrepancy is likely due to the differences in optimal processing parameters which are dictated by the feed rod's size and material. To further confirm whether the deposition was useful, several tests were conducted on the deposition and substrate and their interface. EDS mapping shows that the composition distribution is uniform across the interface without apparent element segregation or new phase formation.

Figure 4(B) shows the interface between the deposited 4140 steel and the 1018 substrate. The interface between the deposition and substrate shows a serrated and interlocking structure, which is common in AFSD due to the extensive deformation of both the substrate and deposited material during deposition [8]. In addition to the existing metallurgical bond between the substrate and deposition, the interlocking microstructure is also expected to augment the strength of the bond through mechanical interlocking. Figure 4(C) shows the hardness across the deposition interface, as well as the hardness of the initial substrate and feed rod materials. Compared to the initial 4140 steel, the deposited material shows a significant increase in hardness from 327.1 ± 11.0 HV to a maximum of 646.6 ± 15.7 HV in the deposit. The increased hardness is directly related to the grain size refinement from the initial feed rod, seen in Figure 4(D), to the deposited material in Figure 4(E); the decrease in the martensitic lathe size and thus increased grain boundary area increases the hardness following Hall-Petch strengthening [9]. The hardness across the interface of the deposition and substrate is abrupt, with the intermediate region between the two materials encompassing less than 250 microns. This matches the microstructure of the interface in

Figure 4(B), where the serrations only extend approximately 20 microns between the deposit and substrate.

Figures 4(F) and 4(G) show the 1018 substrate microstructure before and after deposition, respectively. The microscopy on the substrate after deposition was conducted 1 mm directly beneath the tool path where the thermal effects would be the greatest. However, due to the relatively low temperatures experienced by the substrate during deposition, the 1018 microstructure remains relatively unchanged. The slight impact on the substrate microstructure from deposition is promising for applications such as repairs where the existing material should not be significantly changed during deposition. Likewise, the hardness of the substrate in Figure 4(C) shows no significant change before and after deposition.

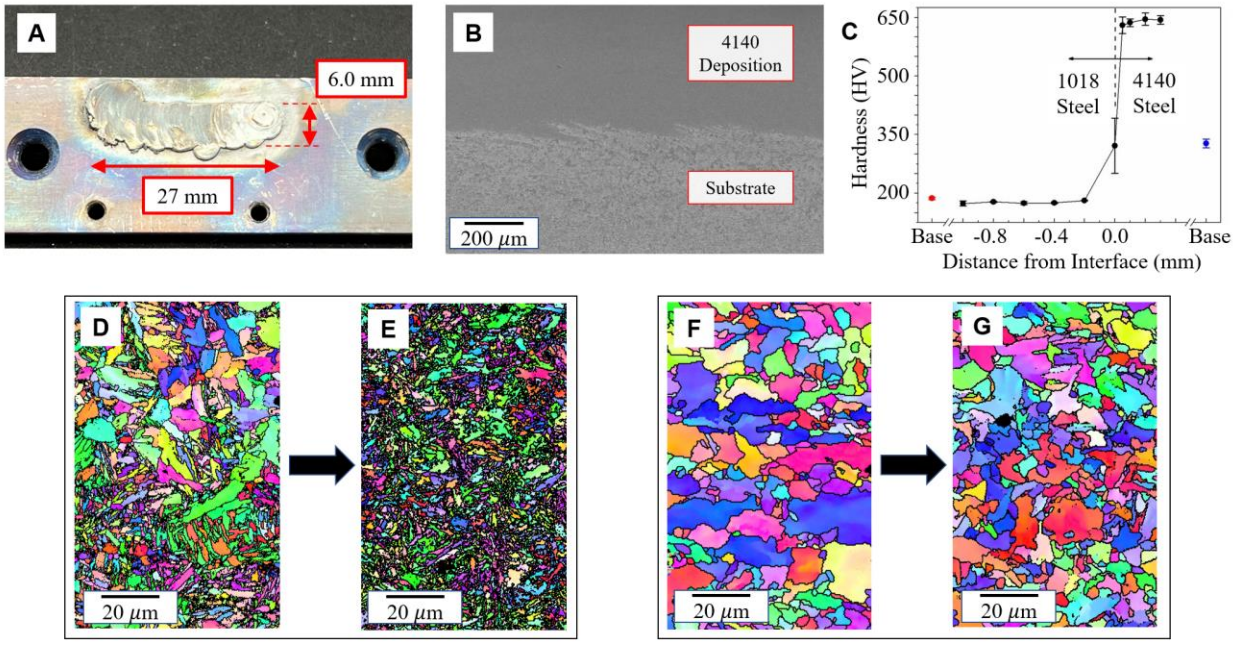

Figure 4. (A) 4140 alloy steel deposition from 2500 RPM, 0.75mm layer height, 60 mm/min traverse speed, and 40 mm/min feed rate. (B) SEM of the interface between the 4140 deposition and the 1018 steel substrate. (C) Hardness across the interface of the deposition also showing the base hardness of the substrate (red) and the 4140 feed rod (blue). (D&E) EBSD of the initial 4140 feed rod (left) and the 4140 post-deposition (right). (F&G) EBSD of the substrate 1 mm below the deposition before (left) and after (right) the deposition.

6. Conclusions and future perspectives

Overall, the modification of the benchtop milling machine to a downsized solid-state additive manufacturing device is promising. The 1 HP motor of the mill was shown to have sufficient speed and torque to deposit even high-strength steel alloys with the addition of 240W of auxiliary induction heat applied to the substrate. The maximum force of 1200 N is a significant reduction from larger scale AFSD, even when accounting for the relative reduction in the area of the feed rod. This makes such a setup attractive for component repair in austere environments. The deposit was of good quality and showed significant grain refinement similar to larger-scale AFSD operations. However, unlike larger-scale AFSD, the heat generated during deposition is very localized and likely results in little weakening of the surrounding substrate.

In future research, more rigorous testing of the system will be conducted. A more comprehensive range of processing conditions needs to be tested to determine their effects on the microstructure and quality of the deposition. Also, a larger track of material should be deposited to allow for direct mechanical testing of the deposited material and the interface. Finally, various other novel feed materials are planned, such as AF96, Haynes 288, and NiTi. It is expected that the advances in the tooling design and thermal management offered by the induction coil heating setup will allow for the deposition of these exotic alloys.

Manuscript 2 References

[1] W.E. Frazier, Metal Additive Manufacturing: A Review, Journal of Materials Engineering and Performance 23(6) (2014) 1917-1928.

[2] J.J. Lewandowski, M. Seifi, Metal Additive Manufacturing: A Review of Mechanical Properties, Annual Review of Materials Research 46(1) (2016) 151-186.

[3] W. Li, K. Yang, S. Yin, X. Yang, Y. Xu, R. Lupoi, Solid-state additive manufacturing and repairing by cold spraying: A review, Journal of Materials Science & Technology 34(3) (2018) 440-457.

[4] H.Z. Yu, R.S. Mishra, Additive friction stir deposition: a deformation processing route to metal additive manufacturing, Materials Research Letters 9(2) (2021) 71-83.

[5] H.Z. Yu, M.E. Jones, G.W. Brady, R.J. Griffiths, D. Garcia, H.A. Rauch, C.D. Cox, N. Hardwick, Non-beam-based metal additive manufacturing enabled by additive friction stir deposition, Scripta Materialia 153 (2018) 122-130.

[6] R.B. Gottwald, R.J. Griffiths, D.T. Petersen, M.E.J. Perry, H.Z. Yu, Solid-State Metal Additive Manufacturing for Structural Repair, Accounts of Materials Research 2(9) (2021) 780-792.

[7] W.D. Hartley, D. Garcia, J.K. Yoder, E. Poczatek, J.H. Forsmark, S.G. Luckey, D.A. Dillard, H.Z. Yu, Solid-state cladding on thin automotive sheet metals enabled by additive friction stir deposition, Journal of materials processing technology 291 (2021).

[8] M.E.J. Perry, R.J. Griffiths, D. Garcia, J.M. Sietins, Y. Zhu, H.Z. Yu, Morphological and microstructural investigation of the non-planar interface formed in solid-state metal additive manufacturing by additive friction stir deposition, Additive Manufacturing 35 (2020) 101293.

[9] W. Sylwestrowicz, E.O. Hall, The Deformation and Ageing of Mild Steel, Proceedings of the Physical Society. Section B 64(6) (1951) 495-502.

3.2 Other Material Systems

While the detailed experiments performed in the previous sections only follow work done with dissimilar steel depositions, several other materials have been tested on this new apparatus to determine how universal the device is. Firstly, to compare to conventional AFSD, aluminum depositions were tested on the machine. Unfortunately, because the device's design requires torque to be transferred through the feed rod to enable stirring in the tool, many aluminum depositions ended with the feed rod twisting and yielding. In addition to this, the heating system was tested to its limits to print nickel superalloys with very high yield strengths, even at elevated temperatures.

The parameters that produced the highest quality depositions for aluminum were a 500 µm layer height, a revolution speed of 2500 RPM, a traversal speed of 30 mm/min, and a feeding rate of 20 mm/min. The deposition, shown in Figure 3, was 25 mm long but had significant gaps in the material filling. The reasoning for this is numerous. Firstly, the aluminum had to be fed extremely

slowly to prevent the material from buckling or twisting under the deposition loading. This caused issues with jamming in every test conducted. Graphite spray was used to coat the feed rod prior to deposition to add a layer of lubrication between the feed rod and tool, but this had little effect. Secondly, aluminum is significantly more thermally conductive than the steel shown previously. This causes the minimal heat generated by friction to rapidly leave the deposition zone resulting in a comparatively cooler deposition. The induction coils added extra thermal energy to attempt to mitigate this, but the heater was incapable of overcoming this issue at the time.

Figure 3. Several attempted aluminum depositions using aluminum 6061 feed rod onto 6061 substrate.

On the other end of the spectrum, depositions were also tested using a nickel superalloy. The materials used in these tests were a Haynes 244 feed rod deposited onto an Inconel 617 substrate. The 617 substrate was chosen due to its use in molten salt reactors to contain liquid salt. This use case requires the material to have high strength at elevated temperatures and be very resistant to the corrosion that molten salt encourages. To bolster both the strength and corrosion resistance of these Inconel pipes, a layer of Haynes 244 could be beneficial. However, deformation-based solid-state additive methods face significant challenges when depositing materials designed for high strength at high temperatures. The process relies on the material becoming soft enough to deform when heated, so materials designed for their strength at elevated temperatures struggle to yield even when heated. Initial work with auxiliary heating could not

deposit anything more than a small button of material. This deposition is shown in Figure 4. To enable proper deposition, the deposition temperature needed to be increased. This necessitated the design of an updated heater, shown in Figure 5. The central part of the heater consisted of a thick low-carbon steel plate which would be heated by the original induction coil from the previous design. External to this was a milled austenitic stainless-steel plate mounted to the mill's bed. This stainless-steel plate had a very low thermal conductivity and was non-magnetic. This heating setup allowed the heat to be concentrated in the central steel plate. On top of the steel plate are a few pin locations and mounting clamps which can hold the same 63.5 x 25.4 mm substrates. When supplied with 24V and 15A of power, this heater design can heat a non-magnetic substrate up to 420 ℃ in 15 minutes, a significant increase over the 220 ℃ of the previous design.

Figure 4. The initial deposition of Haynes 244 onto Inconel 617 using the original auxiliary heater with a peak preheating temperature of 220 ℃.

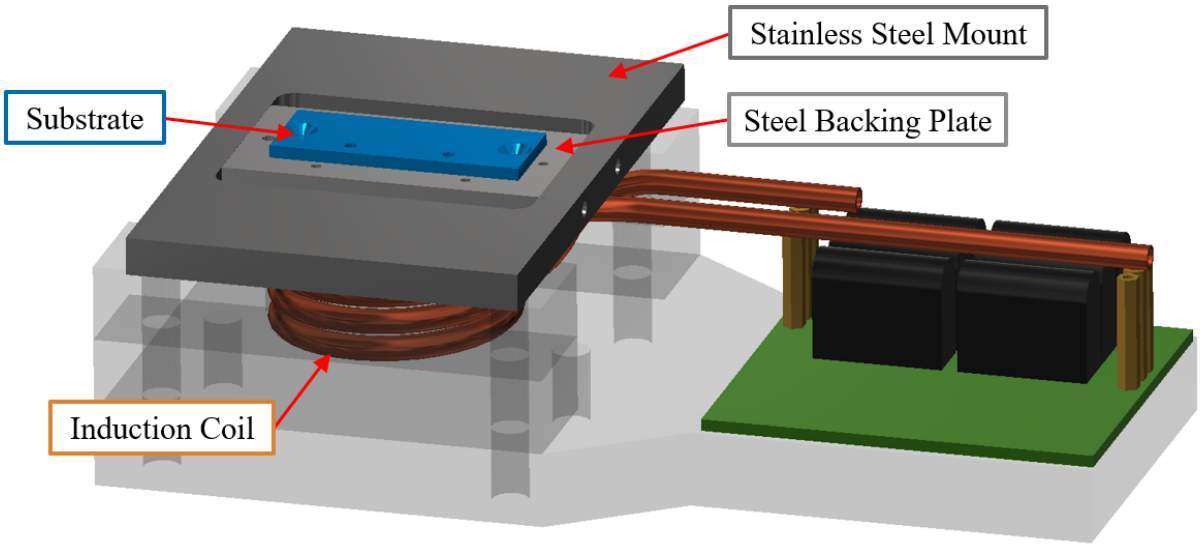

Figure 5. (a) Updated heater mechanism with a two-part steel and stainless-steel design.

Utilizing this increase in temperature, a proper deposition track of Haynes 244 was created. The deposition parameters were an initial feed rate of 5 mm/min, a constant speed of 2500 RPM, a 750 µm layer height, 72 mm/min traverse, and 48 mm/min deposition feed. The deposit, shown in Figure 6, was only 13 mm long but a marked improvement from previous depositions and proof that the material can be processed both by solid-state methods and by this downscaled approach. A similar hardness plot to that presented for the steel is shown in Figure 7. As seen before, there is relatively little change in the hardness of the substrate, while the deposition has a hardness that is significantly increased compared to the base feed material. Finally, an image showing a cross-sectional view of the deposit along the deposition direction is presented in Figure 8. Of note, there is significant mixing between the substrate and feed material, especially near the beginning of the deposition. There is a thin layer at the interface which may be inadequate bonding between the layers. Likely, the temperature was not high enough as deposition continued indicating that the traversal speed was too high, so there is room for future advancements.

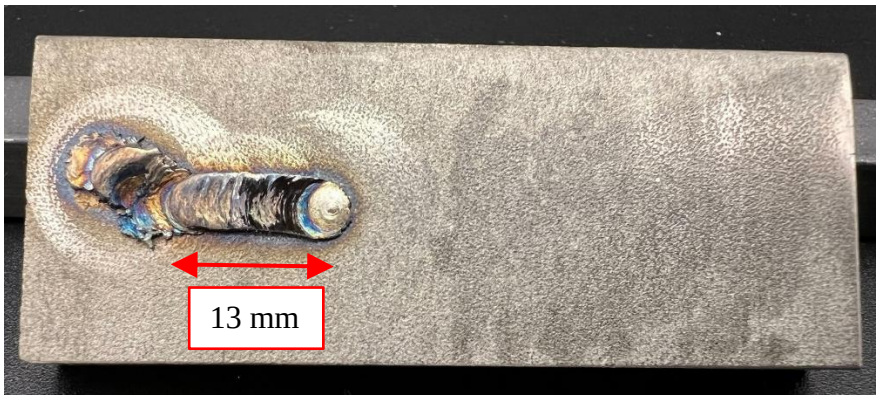

Figure 6. Updated deposition of Haynes 244 onto Inconel 617 with the advanced heater design with a peak preheating temperature of 420 ℃.

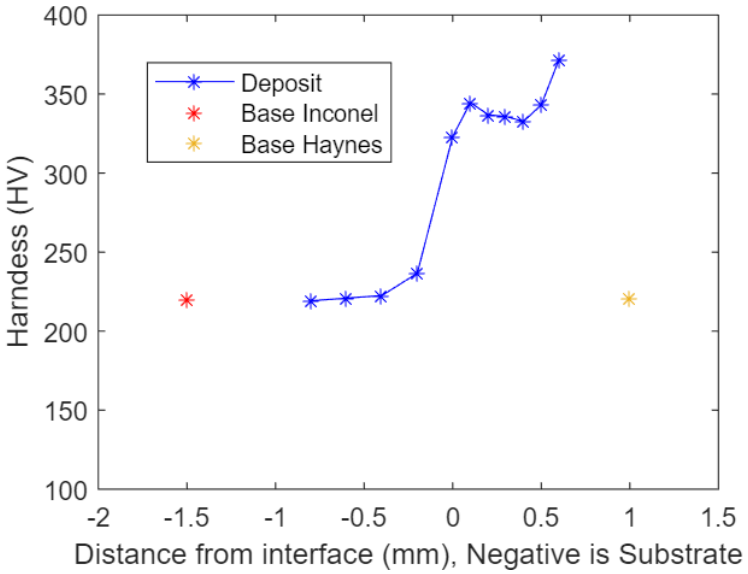

Figure 7. The hardness of the Haynes 244 on Inconel 617 deposition across the interface. The red and yellow data points correspond to the base hardness of the Inconel and Haynes, respectively.

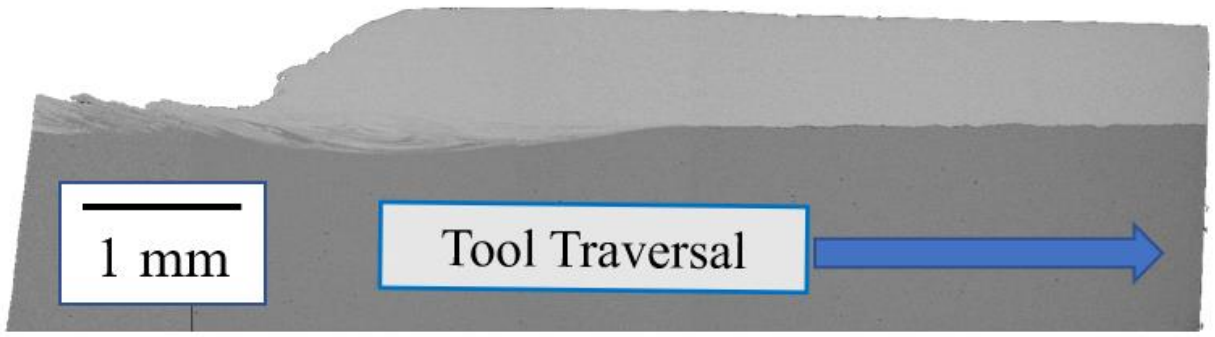

Figure 8. Cross-section view of the Haynes 244 deposition on the Inconel 617 substrate. The arrow shows the direction of travel for the tool.

3.3 Feeding Mechanism Upgrades

As noted through the result sections, several pervasive issues affect the quality of the depositions. Many of the problems presented thus far revolve around either incomplete material filling or insufficient heating. However, the machine's success rate is relatively low due to various factors dictating whether the tool will jam during deposition. There is considerable room for improvement in the machine's ability to produce quality depositions, especially in high-strength materials such as steel. One major pitfall of the existing design is using a single bearing to support the deposition tool. The sideways movement during deposition creates a significant moment that the bearing is not designed to support. This often leads to jamming in the tool if the drag from the material flow surpasses a critical force. Additionally, the use of the support structure creates another large moment arm for the forces of the tool to act. The high forces during deposition can deflect the structure, which is effectively a cantilevered beam, by several millimeters. This adversely affects both the visual and mechanical qualities of a deposition. If the tool shifts too much relative to the deposition, it is forced to extrude material on an unheated substrate which is likely to spike the feeding force and cause a jam. Thus, to address many of these issues, a more robust method to hold the tool is needed. A promising approach would be to use the mill’s existing structure.

A proposed modification to the feeding mechanism, shown below in Figure 9, was created to accomplish this. By moving the feeding mechanism to the top of the mill and not using the mill's quill feed like was done previously, the tool can be held in the mill's collet like a typical cutting tool. This leverages the inherent rigidity in the mill. This setup of the feeding mechanism pushing from the top was not previously possible as there was no way to access the back of the feed rod if the tool were held in the collet. To overcome this, a custom hollow drawbar was created for the milling machine that allows a circular push rod to move along the axis of rotation of the mill's spindle. By forcing this circular push rod downward with a couple of stepper motors fastened to ball screws, the downward movement of the feed rod can be controlled identically to before. Additionally, by moving the tool into the spindle, the torque supplied to the tool no longer needs to be transferred through the feed rod. This significantly improves the deposition of weaker alloys, like aluminum and copper.

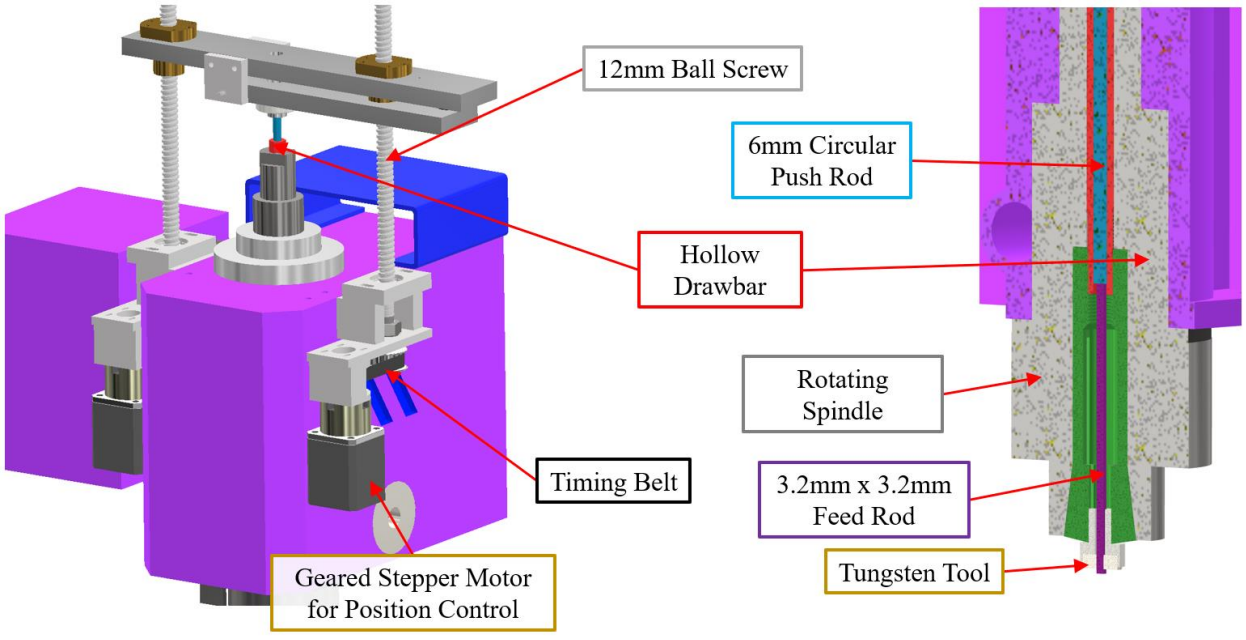

Figure 9. Redesign of the downscaled solid-state additive manufacturing feeding mechanism that allows for a significantly more robust tool-holding setup.

A single deposition of aluminum 6061 was conducted to test the effectiveness of this new setup. In addition to the upgraded feeding mechanism and tool holding, the upgraded heater was also used for this deposition. Specifically for aluminum, the preheat temperature of 420 ℃ is quite significant. This is in the realm of the temperature needed for deposition without any frictional heating. For this metal, in particular, there is a promising research opportunity to explore how the revolution speed affects the deposition quality practically independent from the heating. With the extra heating, different machine parameters could be used. These were a 750 µm layer height, a revolution speed of 1425 RPM, a traversal speed of 45 mm/min, and a feeding speed of 30 mm/min. The initial feeding rate was set to 5 mm/min as well. The results of this deposition, seen in Figure 10, show that this machine is considerably more capable of processing aluminum alloys than the previous setup. The deposition runs from left to right in the image shown. It is slightly underfilled at the beginning, resulting in some periodic gaps in the surface. However, in the center of the deposit, the surface is quite smooth and does not show a strong preference between the advancing and retreating edges of the tool. In general, the upgraded machine has expanded capabilities compared to the original feeding mechanism and can further expand upon the exploratory research into downscaled solid-state additive manufacturing presented here.

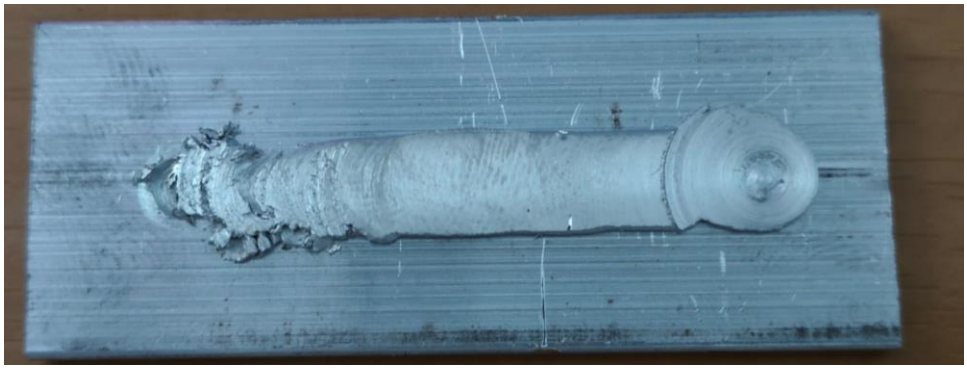

Figure 10. Aluminum 6061 feed rod on aluminum 6061 substrate deposition using the upgrade mill feeding mechanism with a preheated temperature of 420 ℃.

Chapter 4: Conclusions and Future Work

Overall, repairing existing components is an untapped need in many circumstances. To varying degrees, difficult-to-weld materials, complex parts, and extensive repairs are challenges that can be addressed by feed-rod-based solid-state additive manufacturing. However, the technology is still new and has many limitations in its current form. The most significant limitations are currently associated with the size of the machines needed to promote deposition. The large size of the machine and feed rod necessitate higher power consumption, axial forces, and component cost. Additionally, the wide depositions and machine weight result in increased material waste and decreased mobility. All of these can be addressed by reducing the size of the feed rod. This avenue had previously yet to be explored, so the feasibility of such a downscaled device needed to be assessed.

Modifying the PM 728VT milling machine into a small solid-state additive manufacturing machine is promising. The 750 W motor on the mill was proven to have adequate torque and speed to promote the deposition of various alloys. These alloys include high-strength steel, aluminum, and even nickel superalloys. This was partly made possible using an auxiliary induction heater setup, increasing the substrate temperature to 420 ℃ before deposition. The maximum force experienced during the steel deposition of only 1275 N significantly decreased from that seen in larger-scale setups, even when considering the reduction in the cross-sectional area of the feed rod. The steel deposit was of good quality and was significantly harder than the base material due to significant grain refinement. Additionally, the heat from the deposition remained very localized beneath the tool, resulting in little softening of the substrate material. A similar device is an attractive solution for the repair of components in austere environments.

For continued research using this machine, a more rigorous design of experiments should be performed to determine the true capabilities of such a setup. Various processing variables should be tested in combination with one another to deduce their individual contributions to the state of the resulting deposition. Additionally, deposition tracks should be layered and joined to create longer and taller deposits to better determine inter-layer strength. This would also allow the deposits to be loaded to assess their strength characteristics directly. More exotic materials are also planned for testing, such as shape-memory nickel-titanium alloys, and the results from these experiments could be of great interest. Finally, an end goal of the project would be to take the mechanical components of what was created and make a truly mobile apparatus by placing the mill head onto a sufficiently sturdy robotic arm.

(Space intentionally left blank)

References

[1] Rahito, D.A. Wahab, A.H. Azman, Additive Manufacturing for Repair and Restoration in Remanufacturing: An Overview from Object Design and Systems Perspectives, Processes 7(11) (2019).

[2] D.H. Phillips, Welding Engineering - An Introduction, John Wiley & Sons, 2016.

[3] C.L. Jenney, A. O'Brien, Welding Handbook, Volume 1 - Welding Science and Technology (9th Edition), American Welding Society (AWS), 2001.

[4] A. O'Brien, K. Sinnes, Welding Handbook, Volume 5 - Materials and Applications, Part 2, 9 ed., American Welding Society2015.

[5] S. Jeong, G. Park, B. Kim, J. Moon, S.-J. Park, C. Lee, Heat-Affected Zone Characteristics with Post-Weld Heat Treatments in Austenitic Fe–Mn–Al–C Lightweight Steels, Metals and Materials International 28(10) (2022) 2371-2380.

[6] B. Onuike, A. Bandyopadhyay, Additive manufacturing in repair: Influence of processing parameters on properties of Inconel 718, Materials Letters 252 (2019) 256-259.

[7] D. Liu, J.C. Lippold, J. Li, S.R. Rohklin, J. Vollbrecht, R. Grylls, Laser Engineered Net Shape (LENS) Technology for the Repair of Ni-Base Superalloy Turbine Components, Metallurgical and Materials Transactions A 45(10) (2014) 4454-4469.

[8] M. Hedges, N. Calder, Near-Net-Shape Rapid Manufacture and Repair by LENS®, Rapid Prototyping 12(4) (2006) 1-13.

[9] L. Wang, S. Felicelli, Y. Gooroochurn, P.T. Wang, M.F. Horstemeyer, Optimization of the LENS® process for steady molten pool size, Materials Science and Engineering: A 474(1) (2008) 148-156.

[10] L. Aucott, H. Dong, W. Mirihanage, R. Atwood, A. Kidess, S. Gao, S. Wen, J. Marsden, S. Feng, M. Tong, T. Connolley, M. Drakopoulos, C.R. Kleijn, I.M. Richardson, D.J. Browne, R.H. Mathiesen, H.V. Atkinson, Revealing internal flow behaviour in arc welding and additive manufacturing of metals, Nature Communications 9(1) (2018).

[11] I. Gibson, D. Rosen, B. Stucker, Additive Manufacturing Technologies, Springer, New York, 2015.

[12] R.S. Mishra, P.S. De, N. Kumar, Introduction, in: R.S. Mishra, P.S. De, N. Kumar (Eds.), Friction Stir Welding and Processing: Science and Engineering, Springer International Publishing, Cham, 2014, pp. 1-11.

[13] K. Petráčková, J. Kondás, M. Guagliano, Fixing a hole (with cold spray), International Journal of Fatigue 110 (2018) 144-152.

[14] H.Z. Yu, R.S. Mishra, Additive friction stir deposition: a deformation processing route to metal additive manufacturing, Materials Research Letters 9(2) (2021) 71-83.

[15] H. Assadi, F. Gärtner, T. Stoltenhoff, H. Kreye, Bonding mechanism in cold gas spraying, Acta Materialia 51(15) (2003) 4379-4394.

[16] J. Cizek, O. Kovarik, J. Siegl, K.A. Khor, I. Dlouhy, Influence of plasma and cold spray deposited Ti Layers on high-cycle fatigue properties of Ti6Al4V substrates, Surface and Coatings Technology 217 (2013) 23-33.

[17] F. Gärtner, T. Stoltenhoff, J. Voyer, H. Kreye, S. Riekehr, M. Koçak, Mechanical properties of cold-sprayed and thermally sprayed copper coatings, Surface and Coatings Technology 200(24) (2006) 6770-6782.

[18] C. Chen, Y. Xie, X. Yan, S. Yin, H. Fukanuma, R. Huang, R. Zhao, J. Wang, Z. Ren, M. Liu, H. Liao, Effect of hot isostatic pressing (HIP) on microstructure and mechanical properties of Ti6Al4V alloy fabricated by cold spray additive manufacturing, Additive Manufacturing 27 (2019) 595-605.

[19] S. Yin, P. Cavaliere, B. Aldwell, R. Jenkins, H. Liao, W. Li, R. Lupoi, Cold spray additive manufacturing and repair: Fundamentals and applications, Additive Manufacturing 21 (2018) 628-650.

[20] H.Z. Yu, M.E. Jones, G.W. Brady, R.J. Griffiths, D. Garcia, H.A. Rauch, C.D. Cox, N. Hardwick, Non-beam-based metal additive manufacturing enabled by additive friction stir deposition, Scripta Materialia 153 (2018) 122-130.

[21] H.Z. Yu, Chapter 1 - Introduction, in: H.Z. Yu (Ed.), Additive Friction Stir Deposition, Elsevier2022, pp. 1-19.

[22] J.K. Yoder, R.J. Griffiths, H.Z. Yu, Deformation-based additive manufacturing of 7075 aluminum with wrought-like mechanical properties, Materials & Design 198 (2021) 109288.

[23] J. Griffiths, D. Garcia, J. Song, V.K. Vasudevan, M.A. Steiner, W. Cai, H.Z. Yu, Solid-state additive manufacturing of aluminum and copper using additive friction stir deposition: Process-microstructure linkages, Materialia 15 (2021).